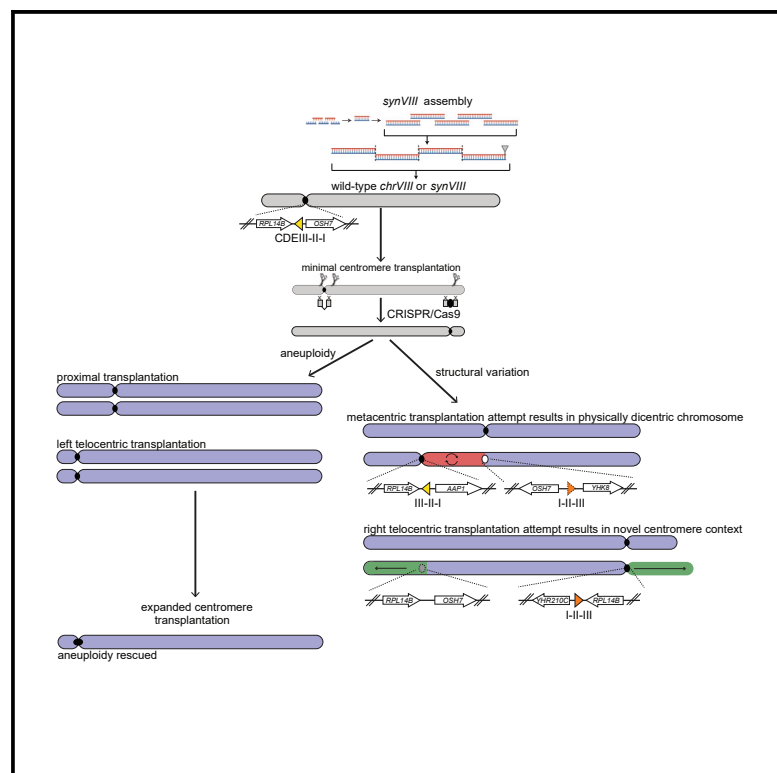# Context-dependent neocentromere activity in synthetic yeast chromosome *VIII*

Graphical abstract

Authors

Stephanie Lauer, Jingchuan Luo,
Luciana Lazar-Stefanita, ..., Joel S. Bader,
Giovanni Stracquadanio, Jef D. Boeke

Correspondence

jef.boeke@nyulangone.org

In brief

Lauer et al. describe assembly and characterization of synthetic chromosome *VIII* (*synVIII*), one of the remaining chromosomes required to synthesize the first eukaryotic genome as part of the international Sc2.0 project. The authors use *synVIII* as a platform for further genome manipulation by relocating the yeast point centromere.

Highlights

- *SynVIII* was completed with wild-type fitness despite many designer modifications

- Minimal 118-bp *CEN8* lacks full function at ectopic locations

- Transplanted minimal *CEN8* led to a physically dicentric chromosome

- Specific pericentromeric sequences are required to improve *CEN8* function

CellPress

Cell Genomics

Article

Context-dependent neocentromere activity in synthetic yeast chromosome *VIII*

Stephanie Lauer,[1,6,8] Jingchuan Luo,[1,7,8] Luciana Lazar-Stefanita,[1] Weimin Zhang,[1] Laura H. McCulloch,[1] Viola Fanfani,[3] Evgenii Lobzaev,[3,4] Max A.B. Haase,[1] Nicole Easo,[1] Yu Zhao,[1] Fangzhou Yu,[1] Jitong Cai,[5] The Build-A-Genome Class, Joel S. Bader,[5] Giovanni Stracquadanio,[3] and Jef D. Boeke[1,2,9,*]

[1]Institute for Systems Genetics and Department of Biochemistry and Molecular Pharmacology, NYU Langone Health, New York, NY, USA
[2]Department of Biomedical Engineering, NYU Tandon School of Engineering, Brooklyn, NY, USA
[3]School of Biological Sciences, The University of Edinburgh, Edinburgh, UK
[4]School of Informatics, The University of Edinburgh, Edinburgh, UK
[5]Department of Biomedical Engineering, Whiting School of Engineering, Johns Hopkins University, Baltimore, MD, USA
[6]Present address: Stephanie Lauer, School of STEM, St. Thomas Aquinas College, Sparkill, NY 10976, USA
[7]Present address: Whitehead Institute for Biomedical Research, 455 Main Street, Cambridge, MA, USA
[8]These authors contributed equally
[9]Lead contact
*Correspondence: jef.boeke@nyulangone.org
https://doi.org/10.1016/j.xgen.2023.100437

SUMMARY

Pioneering advances in genome engineering, and specifically in genome writing, have revolutionized the field of synthetic biology, propelling us toward the creation of synthetic genomes. The Sc2.0 project aims to build the first fully synthetic eukaryotic organism by assembling the genome of *Saccharomyces cerevisiae*. With the completion of synthetic chromosome *VIII* (*synVIII*) described here, this goal is within reach. In addition to writing the yeast genome, we sought to manipulate an essential functional element: the point centromere. By relocating the native centromere sequence to various positions along chromosome *VIII*, we discovered that the minimal 118-bp *CEN8* sequence is insufficient for conferring chromosomal stability at ectopic locations. Expanding the transplanted sequence to include a small segment (∼500 bp) of the *CDEIII*-proximal pericentromere improved chromosome stability, demonstrating that minimal centromeres display context-dependent functionality.

INTRODUCTION

The Synthetic Yeast Genome Project (Sc2.0) aims to build the first eukaryotic genome, marking a groundbreaking achievement in the field of synthetic biology. With the assembly of synthetic chromosome *VIII* (*synVIII*) and additional chromosomes described in this collection of papers, all designer *Saccharomyces cerevisiae* chromosomes are complete.[1–11] Previously published chromosomes include *synIXR*, *synIII*, *synV*, *synVI*, *synII*, *synX*, and *synXII*,[12–18] which have since been consolidated into a single strain along with *synIV*.[1]

DNA synthesis technologies have advanced rapidly in the past 20 years, enabling the synthesis of entire genomes.[19] Early genome synthesis projects precisely replicated existing genomes or incorporated short, synonymously recoded nucleotide "watermarks" to distinguish synthetic sequences from native DNA (reviewed in Zhang et al.[20]). Recently, researchers have focused on building more complex genomes with additional designer modifications and new features. For example, codon reassignment[21,22] and genome minimization have been performed successfully in bacteria.[23,24] Sense and stop codon reassignment in *E. coli* enabled incorporation of noncanonical amino acids into proteins.[25] Completion of a synthetic yeast genome has similar applications but also answers fundamental biological questions specific to eukaryotes. Sc2.0 provides a platform to investigate the essentiality of the RNA splicing machinery, to determine the consequences of whole-genome rearrangements (including creation of minimal yeast genomes) generated through the inducible evolution system SCRaMbLE (synthetic chromosome rearrangement and modification by LoxP-mediated evolution), and to evaluate how complex features such as telomeres, tRNA genes, and rDNA loci change gene expression profiles and genome architecture upon transplantation.[3,26–28]

To continue exploring genome manipulation of functional elements in the context of the Sc2.0 project, we used the recently completed *synVIII* strain as a framework for relocating the centromere and monitoring the effects of such manipulation. The point centromere of budding yeast, which is only 112–120 base pairs (bp) in length, is essential for faithful chromosome segregation and can be defined by consensus DNA elements *CDEI*, *CDEII*, and *CDEIII*.[29] Whereas kinetochore assembly is mediated by recruitment of proteins and protein complexes that bind directly to these consensus sequences, adjacent pericentromeric DNA plays an important role. Sister chromatid

cohesion depends on organization of condensin and cohesin, localization of which is restricted spatially by convergent gene pairs in the pericentromere.[30] Chromosome segregation also depends on DNA looping and formation of specific three-dimensional pericentric structures.[31,32] Transcription initiation of centromeric RNAs, which epigenetically regulate centromere function, occurs in adjacent pericentric sequences.[33–35] Taken together, these findings illustrate the emerging view that pericentromeric sequences may be important for function and regulation of the point centromere.

It is well established that point centromeres of budding yeast can maintain functionality outside of their original context. Ectopic function has been reported for a 627-bp sequence containing *CEN3*, a 125-bp sequence containing *CEN6*, and an 858-bp sequence containing *CEN11*.[29,36–38] Replacing *CEN3* with the 858-bp *CEN11* sequence does not affect the stability of chromosome *III*, suggesting that centromeres are interchangeable.[39] Importantly, the 125-bp DNA sequence containing *CEN6* is sufficient for centromere function on both circular and linear chromosome fragments.[38] That same 125-bp *CEN6* sequence is a component of the plasmid shuttle vectors widely used by the yeast community.[40] These results suggest that point centromere functionality can be achieved without specific flanking pericentric sequences. However, it is unknown whether this finding can be extended to other centromeres in different chromosomal contexts. Relocating the budding yeast centromere to various positions along a single chromosome (*VIII*) enabled us to directly test the suitability of several ectopic destinations for centromere function and stability.

In this study, we used single-step intrachromosomal centromere transplantation (SSICT) to transplant the minimal 118-bp *CEN8* sequence (defined here as extending from the first base of *CDEI* to the last base of *CDEIII*) to four ectopic positions along synthetic and wild-type chromosome *VIII*. Two transplantation attempts resulted in structural variations that led to either formation of (1) a hybrid centromere that retained its *CDEIII*-proximal pericentromeric context or (2) a physically dicentric chromosome in which the intact transplanted centromere sequence appears to be inactive. The apparently successful transplantation of minimal *CEN8* (i.e., without introducing structural variation) to two other target locations led to chromosome *VIII* aneuploidy that was stably maintained despite efforts to forcibly lose the aneuploid chromosome. We interpret the aneuploidy as resulting from incomplete centromere function, resulting in nondisjunction and subsequent accumulation of an extra copy of chromosome *VIII*. This phenomenon appears generalizable to at least one other chromosome and centromere, as it was observed in different strain backgrounds and during an independent experiment to simultaneously delete *CEN9* and integrate *CEN1* at an ectopic position on chromosome *IX*. To uncover the basis for stable aneuploidy in centromere-relocated strains, we used a circular *CEN8*-containing minichromosome to test stability in the presence and absence of pericentromeric sequences. We found that the minimal 118-bp CEN8 sequence led to high plasmid loss rates that were rescued when specific pericentromeric sequences proximal to *CDEIII* were included. Finally, using this improved version of *CEN8*, we were able to vastly enhance SSICT, mostly eliminating the aneuploidy associated with centromere transplantation.

RESULTS

Design, synthesis, and assembly of *synVIII*

In this study, we report the completion of synthetic chromosome *VIII*, or *synVIII*, which was designed as part of the Sc2.0 project. *SynVIII* measures 504,827 bp in length, which is about 60 kb or 10.3% shorter than wild-type *VIII* (562,643 bp; Figure S1). Assembly of *synVIII* involved the most hierarchical bottom-up strategy for chromosomes in the Sc2.0 project, as *synVIII* is the only synthetic chromosome having all four types of intermediate DNA products that lie between synthetic oligonucleotides and full chromosomes: building blocks, minichunks, chunks, and megachunks (Figure 1A).

Designer *synVIII* has specific features common to all Sc2.0 chromosomes.[42] One goal of the Sc2.0 project is to increase genome stability while retaining wild-type levels of fitness. In budding yeast, tRNA genes tend to lie adjacent to long terminal repeat (LTR) sequences, which are thought to lead to replication fork blockage and collapse, promoting genome rearrangement via flanking homologous sequences such as Ty elements and/or the tRNA genes themselves, most of which represent dispersed repeats. Accordingly, all 11 tRNA genes and the associated LTRs were removed. The 11 tRNA genes were relocated to a tRNA neochromosome, which has been constructed and will be incorporated into the final Sc2.0 genome.[11] The original telomere regions were replaced by a 300-bp universal telomere cap sequence, previously shown to be functional.[12,13,43] During this process, subtelomeric repeats were deleted. All introns, including one in an essential gene, were also removed. All TAG stop codons were recoded to TAA (Figure 1B). Finally, to increase genomic flexibility and enable use of the inducible evolution system SCRaMbLE,[12,27,44] 183 loxPsym sites were added to the 3′ UTR of each nonessential gene and at or adjacent to several unique genomic landmarks, including the centromere and telomeres.

To build *synVIII*, megachunks were integrated using switching auxotrophies progressively for integration (SwAP-In), a method that utilizes homologous recombination to sequentially replace tracts of wild-type sequence with synthetic DNA, alternating auxotrophic marker genes with each integration (Table S1). In addition, we used a meiotic parallelization strategy, similar to what was used for *synXII* and *synIV*.[3,18] In brief, several semisynthetic versions of *synVIII* were built in parallel in discrete strains with different mating types. By mating two semi-synthetic strains that carry different auxotrophic markers and contain overlapping *synVIII* sequences, we facilitated homologous recombination between their homologs during meiosis. This approach permitted replacement of wild-type chromosome *VIII* sequences with synthetic fragments in three different initial strains simultaneously, enabling efficient assembly and debugging of *synVIII* (Figure S2).

Whole-genome sequencing (WGS) and analysis of the resulting *synVIII* strain revealed that the majority of synthetic sequences were successfully integrated. However, sequencing coverage across *synVIII* revealed a 30-kb duplication within megachunk G (Figure 1C). This duplication was repaired using a two-step CRISPR editing strategy, similar to one described previously,[15] in which half of each duplicate copy is replaced
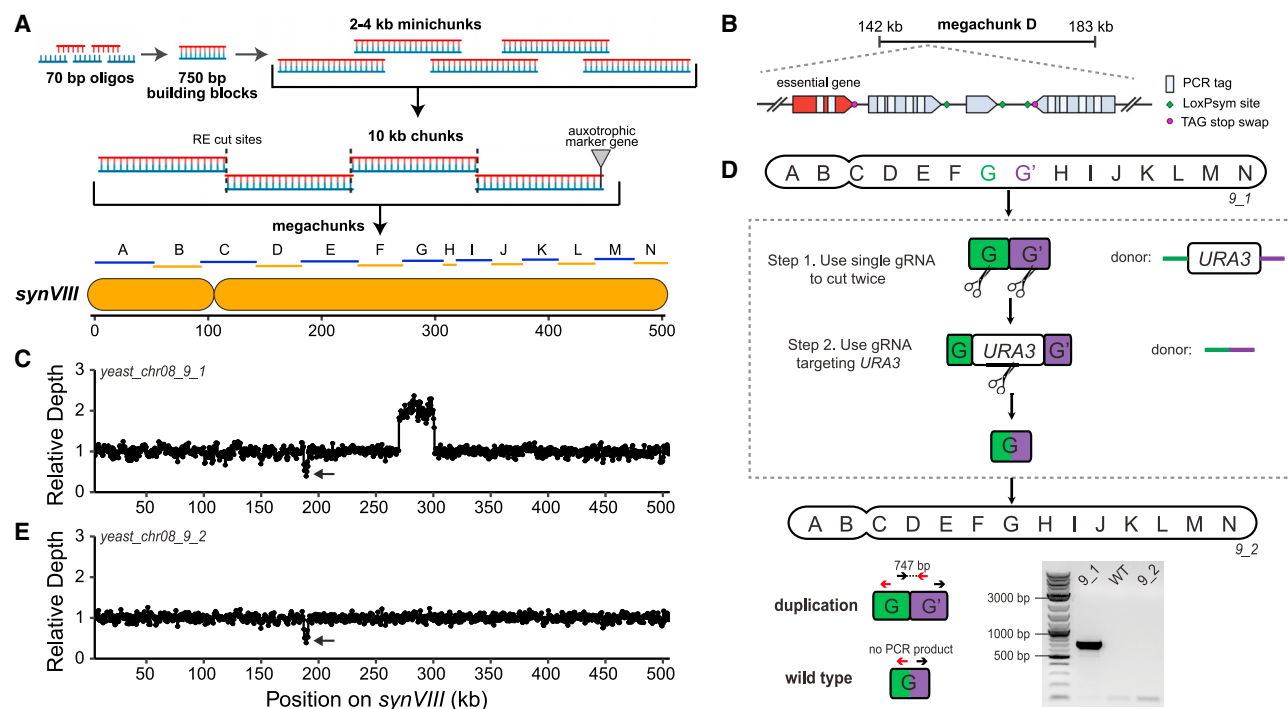
Figure 1. Design and assembly of *synVIII*

(A) SynVIII hierarchical assembly workflow. Building blocks, assembled from overlapping ~70 bp oligonucleotides as part of Sc2.0's Build-A-Genome course, were used to generate single minichunks ranging from ~2 to 4 kb in size. Homologous recombination between overlapping minichunks[41] resulted in ~10-kb chunks that were ligated together after restriction enzyme digestion to form megachunks A–N. oligos, oligonucleotides; RE, restriction enzyme; bp, base pairs; kb, kilobase pairs.

(B) Schematic representation of several Sc2.0 design features within megachunk D. An essential gene (red) does not contain a loxPsym site in the 3′-end of the UTR.

(C) WGS analysis revealed a duplication in megachunk G.

(D) The duplication was repaired using a two-step CRISPR-Cas9 approach. Paired red and black arrows indicate the approximate binding locations of primers that bind two distinct locations in strains with the duplication. PCR results shown are representative of five technical replicates. WT, wild type.

(E) Removal of duplicate sequences restored the read depth profile. (C, E) Read depth was calculated for non-overlapping 500-bp windows and normalized to the median depth across the chromosome. Arrows represent decreased sequencing depth at the *CUP1* locus, which is present in single copy in *synVIII* but present in multiple copies in wild-type yeast and the S288C reference.

by a *URA3* marker gene that is subsequently removed (Figure 1D). Candidates were screened by PCR and verified by WGS analysis. Coverage across the chromosome indicated that megachunk G was present in one copy, confirming that the duplication was removed (Figure 1E). Repairing the duplication did not affect strain fitness, indicating that the duplication probably arose spontaneously during assembly and not as a consequence of selection for fitness improvement (Figure S3).

After several additional rounds of CRISPR-Cas9 editing, yeast_chr08_9_1 was updated to a final version, yeast_chr08_9_11 (Table S2). During this process, ~25 kb of missing synthetic sequence corresponding to megachunk C was integrated (Figure S4). Additional modifications were made to the living strain in response to an updated version of the S288c reference, although there was no obvious fitness defect associated with these mutations (Table S3). Two unintended mutations in coding regions were repaired including one frameshift mutation in *TDA3* (discussed below, Table S4). All modifications were verified by WGS.

Characterization of *synVIII*

Characterization of a draft *synVIII* strain revealed wild-type levels of growth on rich media at 30°C and 37°C (Figure S5). However, growth rates were decreased at 22°C and 25°C compared with wild-type yeast (Figure 2A). This phenotype was more pronounced in *synVIII_9_4* (yeast_chr_08_9_4) and intermediate strains, where we used CRISPR-Cas9 to perform stepwise integration of missing synthetic minichunks within megachunk C. This stepwise integration enabled us to pinpoint the cause of the defect: an unintended 1-bp deletion in the gene *TDA3*. This deletion results in a frameshift early in the coding sequence, presumably rendering the protein nonfunctional. In accordance with this, a *TDA3* knockout strain had a similar growth defect at 22°C (Figure 2B). After repairing *TDA3*, *synVIII* grew comparably with wild-type yeast under eight different standard conditions (Figure 2C) and 15 other conditions (Figure S6).[13]

Comparison of RNA sequencing data with the wild-type strain BY4741 revealed few changes to gene expression across the *synVIII* chromosome (Figure 2D). Several of the genes that are
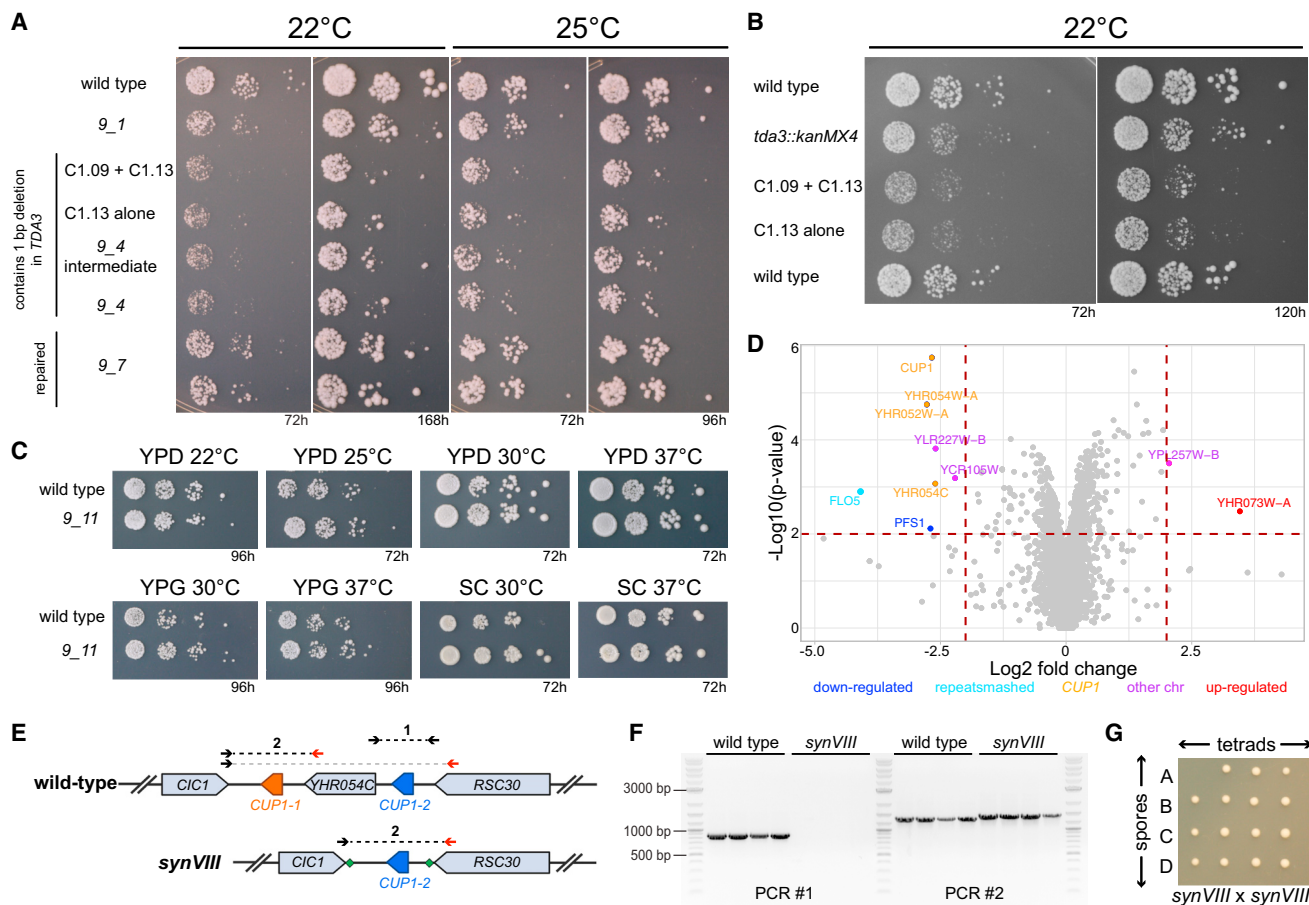
Figure 2. Debugging and characterization of *synVIII*

(A—C) 10-fold serial dilution spot assays of *synVIII* strains, with BY4741 serving as a wild-type control. (A) Minichunk C1.13 contains a 1-bp deletion in the gene *TDA3*, which leads to a fitness defect on YPD medium at 22°C and 25°C in strains that contain the minichunk and yeast_chr08_9_4, which contains all of megachunk C. (B) The fitness defects observed on YPD medium at 22°C for *synVIII* are similar to defects observed in a *tda3* knockout that is otherwise genetically identical to BY4741. (C) The final version of *synVIII*, yeast_chr08_9_11, which includes the repaired version of *TDA3*, grows comparably well with wild-type yeast under eight different growth conditions. YPD, yeast extract peptone dextrose; YPG, yeast extract peptone glycerol; SC, synthetic complete.

(D) Volcano plot illustrating gene expression differences between *synVIII* and BY4741. Upregulated genes on chromosome *VIII* are in red and downregulated genes on chromosome *VIII* are in blue. *FLO5* is a "repeat-smashed" gene shown in teal (these genes were pervasively recoded using GeneDesign's RepeatSmasher[42,45] and thus do not provide accurate RNA-seq data), *CUP1* and associated genes are in yellow, and DEGs on other chromosomes are in purple. The fold change cutoff is 4, with a p value cutoff of 0.01.

(E) Schematic illustration of the *CUP1* locus with arrows representing primers used for diagnostic PCR. The red arrow indicates a primer that binds in two distinct locations due to the presence of homologous sequence.

(F) Diagnostic colony PCR demonstrates that *YHR054C* is deleted. Four independent colonies were tested for each strain.

(G) A diploid homozygous for *synVIII* creates viable spores after tetrad dissection.

differentially expressed reflect intended Sc2.0 design changes. For instance, the copper metallothionein *CUP1* and adjacent genes show low signal as expected; the wild-type reference contains two copies of the *CUP1* locus, while *synVIII* contains only a single copy, verified by diagnostic PCR and Sanger sequencing (Figures 2E and 2F). In addition, diploid strains homozygous for *synVIII* are capable of undergoing sporulation, and dissected tetrads are viable (Figure 2G). Because there are relatively few changes to gene expression and the strain achieves wild-type levels of growth under a variety of conditions, we conclude that the designer features of *synVIII* do not compromise cell fitness.

Engineering neocentromeres by directed transplantation

After successful assembly and characterization of *synVIII*, we aimed to further manipulate the chromosome by relocating an essential functional element: the point centromere. A CRISPR-Cas9 approach was used to simultaneously delete native *CEN8* (n*CEN8*) and re-insert it at various ectopic positions (e*CEN8*) along both synthetic and wild-type chromosome *VIII* (Figure 3A). Specifically, we transplanted the 118-bp sequence that ranges from the first base of *CDEI* to the last base of *CDEIII* and refer to it here as the minimal *CEN8* sequence. On chromosome *VIII*, *CDEI* is attached to the right arm of the chromosome,
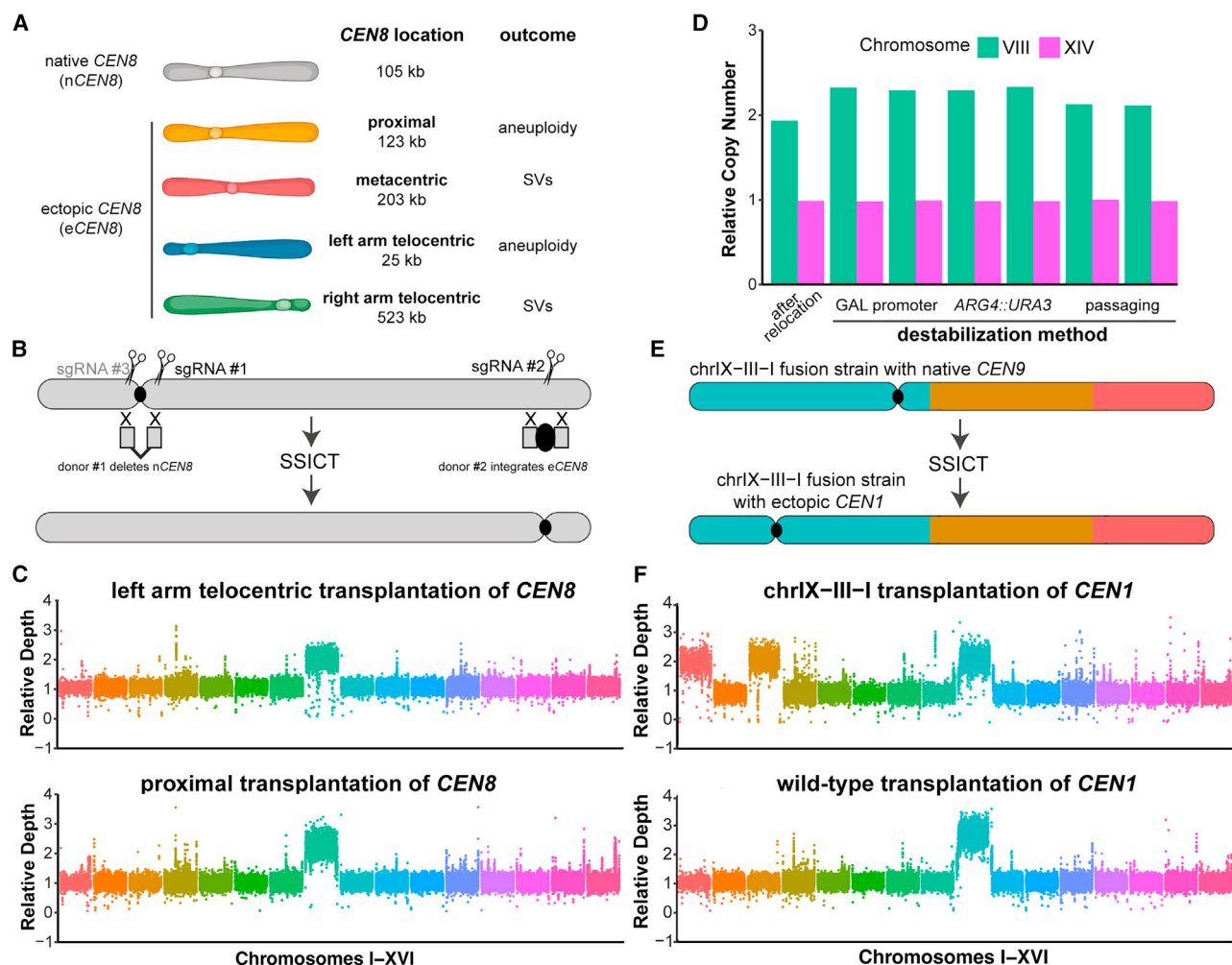
Figure 3. Centromere transplantation via SSICT results in persistent aneuploidy regardless of strain background or position

(A) Schematic illustration of ectopic centromere positions on chromosome *VIII* and the outcomes of successful SSICT at each position. SV, structural variant.

(B) Schematic representation of the SSICT method, which uses two to three sgRNAs targeting native and ectopic positions to simultaneously delete n*CEN8* and integrate e*CEN8* via homologous recombination.

(C) Read depth profiles analyzed from WGS data indicate that *chrVIII* is present in two copies after successful SSICT for two representative strains. Results are similar for left arm telocentric transplants in the wild-type background and proximal transplants in the *synVIII* background; see Table S5.

(D) Three different methods were used to attempt to destabilize or lose the aneuploid chromosome of the left arm telocentric e*CEN8* strain ySLL260. Copy number was calculated by dividing the median depth of each chromosome by the median depth of the genome.

(E) Schematic illustration of fusion chromosome *IX-III-I* generated in Luo et al.[46] before and after SSICT. Different colors represent each chromosome: *chrI* (red), *chrIII* (gold), and *chrIX* (teal).

(F) Read depth profiles analyzed from WGS data indicate that *chrIX-III-I* in the fusion strain and *chrIX* in the wild-type background are present in two to three copies. (C and F) Relative depth was calculated by determining the median read depth, calculated from reads per position, across each chromosome relative to the genome average. Reads were randomly downsampled, and plots were modified for presentation purposes.

and *CDEIII* is attached to the left arm. The initial target locations (metacentric and right arm telocentric) were chosen by inserting centromeres at the midpoint of long intergenic regions (gene deserts), flanked by nonessential genes. Subsequently, we chose additional sites that would produce chromosomes that were left arm telocentric or close to the original *CEN8* location (proximal), replacing nearby dubious open reading frames *YHL037C* and *YHR007C-A*, respectively. This relocation strategy, SSICT, involves co-transformation of two to three distinct single guide RNAs (sgRNAs) that guide Cas9 to target both the native centro-

mere and the target insertion site. Double-strand breaks arise at both targeted locations, and homology-directed repair occurs with co-introduced linear donor DNA fragments (Figure 3B).

Persistent aneuploidy is observed in strains with transplanted minimal CEN8

After an initial PCR screen, centromere transplantations were confirmed by WGS analysis used to detect structural variants since centromere transplantations can be visualized as intra-chromosomal translocations. Successful transplantation of a minimal 118-bp *CEN8* sequence resulted in *chrVIII* aneuploidy

(or structural variants, see below) in both wild-type and synthetic strains regardless of its position (Figure 3C). In these strains, both copies of the chromosome carried the translocated centromere and lacked the native centromere. For the left arm telocentric transplantation, wild-type and synthetic chromosome *VIII* had an average of 1.4× and 2× coverage, respectively, compared to 1× coverage on other chromosomes such as *XIV* (Figure 3D after relocation; Table S5). That is, by sequence coverage, these appear to be disomic haploid strains. We applied three different strategies to try to selectively destabilize the aneuploid chromosome: (1) galactose induction after integration of a chromosome-destabilizing cassette consisting of a *URA3* gene and a *pGAL* promoter inserted adjacent to *CEN8* on one copy of *chrVIII*, followed by 5-FOA selection to produce monosomes,[47,48] (2) replacement of the *ARG4* gene with *URA3* on one copy of *chrVIII to* produce an Arg⁺ strain, with subsequent 5-FOA selection to produce monosomes, and (3) repeated passaging in rich medium (STAR Methods). The *pGAL-CEN* system has been used explicitly for chromosome destabilization during the construction, debugging, and consolidation of synthetic chromosomes in the Sc2.0 project.[1,5,16] Surprisingly, none of these methods resulted in chromosome *VIII* euploidy (Figure 3D, destabilization; Table S5). Similar results were obtained when the chosen ectopic destination was proximal to the original centromere (Table S5). This persistent aneuploidy suggests that the minimal 118-bp *CEN8* sequence leads to chromosome instability via high rates of nondisjunction at two ectopic locations on synthetic and wild-type chromosome *VIII*.

In an independent experiment, we used SSICT to simultaneously delete native *CEN9* and then integrate minimal *CEN1* at an ectopic position (a "gene desert" at *chrIX*: 174,102; Figure 3E). These experiments were performed both in the wild-type strain BY4741 (lower panel) and in a strain where chromosomes *IX*, *III*, and *I* had previously been fused using a CRISPR-Cas9-based strategy (upper panel).[46] Importantly, *CEN1* was previously deleted by design in the *IX-III-I* fusion chromosome, thereby eliminating homologous sequences and subsequent potential recombination between the donor DNA and native *CEN1*. Successful SSICT in either strain background resulted in aneuploidy, dramatically visible in the case of the *IX-III-I* fusion chromosome, where coverage of all three chromosomes simultaneously increases up to ~2, suggesting that this behavior is not a unique feature of minimal *CEN8* but may be a general feature of minimal centromeres (Figure 3F and Table S6). However, it is formally possible that the aneuploidy is a consequence of introducing neocentromeres by SSICT, a possibility we subsequently eliminated, as will be described in a later section of this paper.

Based on these results, we hypothesized that the minimal centromeres we are trying to transplant are in fact not fully functional, but their consequent partial loss of function leads to a mixture of disomic and monosomic strains, primarily maintained by selection for the disomic state. A high rate of nondisjunction typical of a partially functional centromere is predicted to give rise to disomic and nullisomic progeny. The latter would be inviable and rapidly removed from the population. Thus, we interpret the intermediate state of "1.5"-ploid as reflecting a mixed population of monosomic and disomic cells that undergo high rates of

nondisjunction resulting from partial centromere activity and rapid and selective death of the nullisomic progeny cells but persistence of disomic cells.

Structural variants that allow stable chromosome ploidy

While SSICT on *chrVIII* resulted in successful transplantation at the proximal and left arm telocentric positions accompanied by aneuploidy, engineering at two other ectopic *chrVIII* loci (Figure 3A, metacentric and right arm telocentric) led to partially successful transplantations that spawned new and very unusual structural variants. Remarkably, one such strain generated after a metacentric transplantation attempt (ySLL223) contains not one but two physical copies of *CEN8*. Earlier studies have documented that plasmids or chromosomes with two centromeres are highly unstable due to their inability to properly disjoin, a phenomenon that can lead to breakage and monocentric derivatives in yeast.[49–51] Because extensive sequencing (including Sanger, WGS) and PCR studies revealed unambiguously that both centromere sequences were present in strain ySLL223, we hypothesized that only one of the two physical centromere copies in this strain was functional as a kinetochore.

The two physical copies of *CEN8* in this strain are separated by an inversion of the intervening chromosomal sequence, which is easily visualized by Hi-C when mapped against the native reference sequence[52] (Figure 4A, lefthand Hi-C map: reads aligned to the wild-type *chrVIII* reference sequence; righthand map: reads aligned to the corrected [partially inverted, indicated by double arrows] sequence in *chrVIII* reference; the full Hi-C map corresponding to the latter is in Figure S7). In this strain, the transplanted copy, e*CEN8*, appears to be nonfunctional as judged by experiments to knock out each centromere individually; whereas native *CEN8* cannot be knocked out, e*CEN8* is readily eliminated (Figure S8). The Hi-C maps confirm that only n*CEN8* appears to be functional, as it shows strong interactions with the other native centromeres (off-diagonal dot in *chrIX* in Figure 4B). Furthermore, n*CEN8* exhibits the pericentromeric "cruciform" 3C/Hi-C pattern typical of an active *S. cerevisiae* centromere.[31] In contrast, e*CEN8* shows neither a cruciform pattern, nor does it show interaction with the other centromeres, and thus it maps far away from the centromere cluster in the 3D model (see native location *CEN8*, yellow dot, and e*CEN8*, orange dot, in Figure 4B and Video S1). Because of the ~100-kb inverted sequence downstream of n*CEN8* (Figure 4A; indicated by black arrowheads), e*CEN8* is flanked by pericentromeric sequences adjacent to *CDEI* and ectopic DNA, generating a "hybrid" centromere context (Figures 4C and 4D). Consequently, n*CEN8* retains its native *CDEIII*-flanking sequence, whereas the *CDEI*-flanking DNA is disrupted by the inversion. Despite this disruption to the original context of n*CEN8*, it retains functionality (Figure S8). These findings are consistent with the hypothesis that only the *CDEIII*-proximal pericentromeric sequence of *CEN8* is required for full function in novel contexts.

In a second strain, the native centromere is correctly deleted, and e*CEN8* is inserted exactly in the proposed destination, but chromosome *VIII* has been converted into an isochromosome with two copies of the left arm and a deletion of ~40 kb of the DNA extending through the right telomere (Figures 4E and 4F). The structure of the isochromosome also provides a "hybrid" centromere context in which pericentromeric sequences from
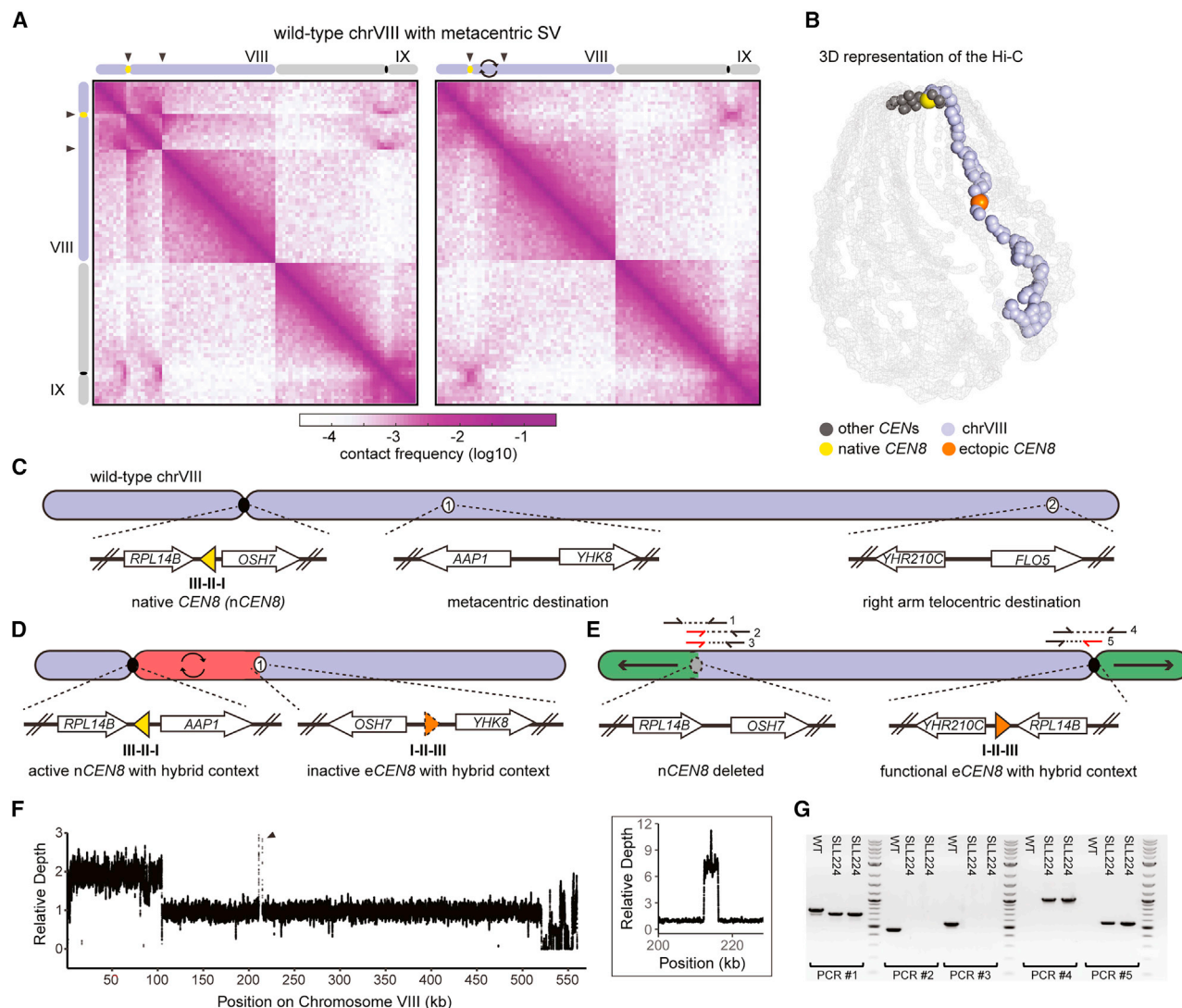
Figure 4. SSICT results in structural variation and hybrid centromere contexts

(A) Two representative insets of Hi-C contact maps for strain ySLL223, obtained after a metacentric transplantation attempt. In the left-hand map, the expected structure of the metacentrically located centromere, designed using the S288C reference sequences of chromosomes *VIII* (light blue; modified to include the ectopic *CEN8* sequence) and *IX* (gray), are schematized; in the right-hand map, the corrected *chrVIII* reference sequence in which the approximate position of the inverted sequence, as revealed by whole-genome sequencing, is indicated by double arrows. The full Hi-C map is included as Figure S7. Schematics of *chrVIII* and *IX* are shown on the *x* and *y* axes; arrowheads indicate left and right end of the intervening inverted sequence between the native and ectopic *CEN8* positions. The Hi-C maps were generated from 5-kb bins; violet to white color scale represented by the right-hand panel reflects high to low contact frequency (log10).

(B) 3D average representations of the right hand Hi-C map in (A). *chrVIII* is shown in light blue, and the inferred native and ectopic *CEN8* positions are colored in yellow and orange, respectively. The remaining chromosomes and centromeres are shown in light gray and black, respectively. See Video S1.

(C) Schematic representation of wild-type *chrVIII* including the native context of *CEN8* and the context of the metacentric and right arm telocentric ectopic positions.

(D) Schematic illustration of the hybrid centromere context accounting for the ~100-kb inversion in strain ySLL223.

(E) Schematic illustration of the hybrid centromere context generated for ySLL224, which was characterized after a right arm telocentric transplantation attempt. Inverted duplication of the left arm forms an isochromosome, a structure confirmed by WGS.

(F) Read depth profile for ySLL224. An absence of reads at the right telomere indicates a deletion, whereas the left arm has been duplicated. Relative depth was calculated by determining the median read depth, calculated from reads per position, across *chrVIII* relative to the genome average. Reads were randomly downsampled, and the plot was modified for presentation purposes. Arrowhead represents increased depth at the *CUP1* locus (inset), which is known to be present in multiple copies in wild-type yeast.

(G) Diagnostic colony PCR provides further evidence for structure of the isochromosome. Two independent colonies of ySLL224 were compared with the wild-type strain BY4741. Red arrows represent primers that bind to *CDEIII* of *CEN8*. WT, wild-type.
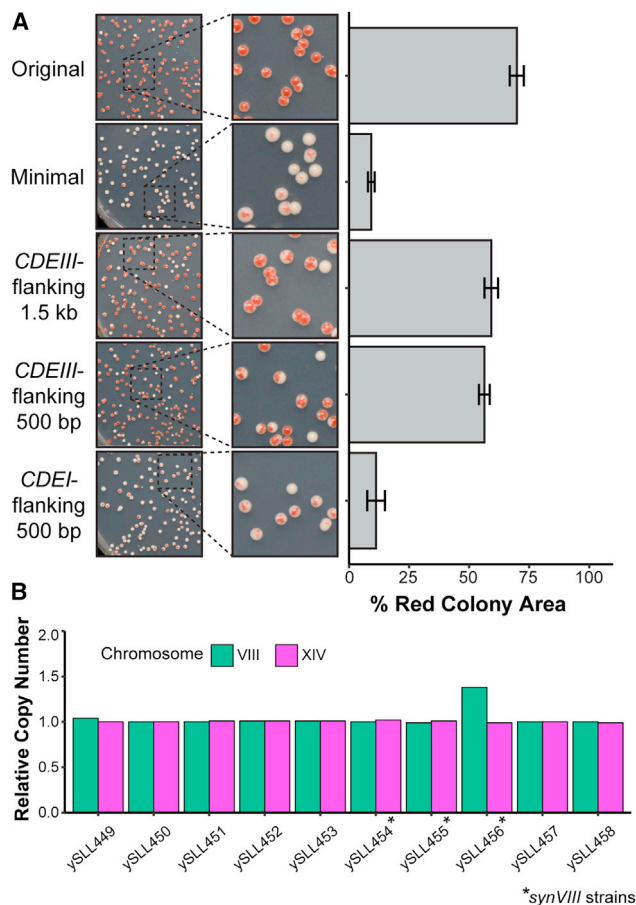
Figure 5. Pericentromeric sequences improve chromosome stability

(A) An *ade2 ade3* derivative of the wild-type strain BY4741 was transformed with *CEN8*-containing minichromosomes, selected and maintained on SC-Ura, and then plated to SC medium with low adenine concentration. Red or partially red colony color shown here on representative SC plates indicates that the minichromosome is maintained, even in the absence of selection. The original construct contains *CEN8* and 5 kb total of pericentromeric sequence, the minimal construct contains only the 118-bp *CEN8* sequence, and the remaining constructs contain 500 or 1.5 kb of pericentromeric sequence. The red colony area was quantified using ImageJ. Averages and standard deviation were calculated from a total of five biological replicates per construct. Raw data are available in Table S7.

(B) Repeating SSICT at the left arm telocentric location with 500 bp of CDEIII-flanking pericentromeric sequence decreased the incidence of *chrVIII* aneuploidy. Copy number was calculated by dividing the median depth of each chromosome by the median depth of the genome.

the *CDEIII*-proximal side of native *CEN8* are retained adjacent to the minimal centromere. The structures of both the physically dicentric and isochromosome variants were verified by diagnostic colony PCR (Figure 4G) and DNA sequencing. These data suggest that *CEN8* functionality may be preserved by the presence of sequences adjacent to *CDEIII*, while the sequences adjacent to *CDEI* are dispensable and result in nonfunctional *CEN8* in certain contexts. Importantly, in both the physically dicentric and isochromosome structural variants, chromosome *VIII* is monosomic, indicating that in these strains, centromere

function in mitotic chromosome segregation is normal (Table S5). A hypothesis for why certain target locations for ectopic centromere function lead to structural variants whereas others give rise to nondisjunction/disomy is provided in the discussion.

Context-dependent function of CEN8

To test our hypothesis that specific pericentromeric sequences are required for *CEN8* function, we used a minichromosome loss rate assay that was developed previously.[34] This assay uses a circular 12-kb minichromosome, WYYYp299 (hereafter described as the original construct), that contains *ADE2* and *URA3* marker genes. In an *ade2 ade3* strain background, maintenance of the minichromosome results in red colonies. During growth under nonselective conditions, the minichromosome can be lost, similarly to a plasmid. Loss of the minichromosome, which can also be described as a failure to segregate efficiently to daughter cells, results in white colonies or partially white colonies that are "sectored" depending on the cell division in which that loss occurs. In the original minichromosome construct, 5 kb total of pericentromeric sequence is present, replicating the context of the point centromere on wild-type chromosome *VIII*.

We modified the original construct to contain only the minimal 118-bp *CEN8* sequence without any flanking pericentromeric sequences. The minimal construct and all other minichromosome constructs described below were verified by whole-plasmid, long-read Oxford Nanopore sequencing. To test minichromosome stability, we plated yeast cells pre-transformed with both constructs on nonselective media and quantified the percent area of red colonies per plate, with a total of five biological replicates per construct. Compared to the original construct in which 70% of the total colony area is red, only 9% of the total colony area is red in yeast harboring the minimal 118-bp *CEN8* construct (Figure 5A). This dramatic decrease in minichromosome maintenance is largely rescued by modifying the construct to include *CDEIII*-proximal pericentromeric sequences. Results were similar for flanking sequences of either 1.5 kb or 500 bp, indicating that 500 bp of *CDEIII*-proximal pericentromeric sequence is sufficient to substantially increase minichromosome stability. In contrast, adding 1.5 kb of *CDEI*-proximal pericentromeric sequence to the minimal *CEN8* construct did not rescue minichromosome stability. Taken together, these data support the hypothesis that pericentromeres, specifically *CDEIII*-proximal pericentromeric sequences within 500 bp, are important for full *CEN8* function.

After identifying pericentromeric sequences that enhance centromere stability, we sought to evaluate whether improved *CEN8* function would be observed in the neocentromere formation assay. We thus repeated SSICT, targeting the left arm telocentric position using a donor with the improved version of *CEN8* containing the extra 500 bp of *CDEIII*-flanking sequence. We identified potential candidates through PCR screening and confirmed successful SSICT for wild-type and synthetic chromosome *VIII* after performing WGS analysis as described above. Of the seven wild-type and three *synVIII* candidates analyzed, one wild-type candidate contained a structural variant on *chrVIII* and one *synVIII* candidate had a relative *chrVIII* copy number of 1.38. The remaining eight candidates were euploid for *chrVIII*, demonstrating that the inclusion of *CDEIII*-proximal pericentric

DNA is sufficient to reduce and nearly eliminate the incidence of aneuploidy during SSICT (Figure 5B), thereby defining an "improved" *CEN8* sequence with regard to transplantability. These results show that SSICT, per se, is not the cause of aneuploidy in the resulting neocentromeric chromosomes but that it is the nature of the centromere fragments used that determines whether centromere function is partial or complete.

DISCUSSION

synVIII assembly and characterization

SynVIII was assembled according to the principles of the Sc2.0 project articulated in previous publications.[12,13,42] Debugging a cold-sensitive phenotype revealed an unexpected frameshift mutation in *TDA3* (*BTN3*), a gene thought to be involved in controlling protein trafficking and replication timing.[53] As is the case with the other synthetic chromosomes, *synVIII* shows a relatively normal transcriptome, with major outliers including *CUP1*, the copy number of which was reduced from two to one in the synthetic strain, and *FLO5*, a gene that was extensively recoded in the process of removing internal tandem repeat sequences. The observation that integration of megachunk C, containing the centromere, was extremely inefficient (an observation echoed by other Sc2.0 members but not documented quantitatively) led us to explore whether centromeres might interfere with integrative recombination. As part of these studies, we decided to transplant the centromere of *synVIII*, forming a "neocentromere" by design. However, our assumption that a minimal sequence including only *CDEI*, *CDEII*, and *CDEIII* would fully support centromere function in an ectopic location was incorrect.

Neocentromere formation led to unexpected structural variations and aneuploidy

Yeast centromeres have three sequence elements (*CDEI, CDEII, CDEIII*) that collectively define the "point centromere" that characterizes all 16 *S. cerevisiae* chromosomes.[29,38,54,55] Two centromeres (*CEN3* and *CEN11*) contain a "*CDEIV*" sequence distal to *CDEIII* and within the pericentromeric sequence identified here.[29] However, we could not find any similarly positioned sequence in any of the other *CEN* sequences or in the centromeres of other *Saccharomyces* species, nor could we find any evidence for the function of this sequence in the literature. Many studies, and indeed, the series of centromeric plasmid vectors in broad use by the yeast community, rest on the widely accepted assumption that the minimal *CDEI-CDEIII* centromere spans just these centromere-defining sequence elements that contain all information needed for mitotic and meiotic centromere function. The evidence for this assumption is substantial and ranges from the sequence conservation itself (and the absence of well-conserved flanking sequence elements) and, most importantly, the stabilizing effect of inserting this minimal *CEN* sequence into plasmids containing a yeast origin of replication or ARS sequence. Two observed effects are consistent with centromere function in these plasmids: (1) segregation of the plasmid from mother cells to daughter cells is dramatically improved: "ARS" plasmids show a dramatic mother cell bias in mitotic cell divisions, and addition of a minimal *CEN* eliminates

this bias. (2) The average copy number of the plasmids is drastically reduced to closer to one copy per cell[38,56] and (mostly) 2:2 segregation in meiosis.[57] However, it is noteworthy that multiple studies have reported that the actual copy number of *CEN* plasmids is closer to three to five copies per cell, and indeed, phenotypes of cells containing yeast genes cloned on *CEN* plasmids are consistent with a "higher than single copy" state.[58–61] Also, studies of 3D genome structure have revealed a very consistent pattern of intrachromosomal pericentromeric interactions associated with native centromeres.[31,62,63] When centromeres are precisely deleted from chromosomes or even inactivated by single base mutations, these pericentromeric chromatin interactions disappear,[64] indicating their dependence on the core centromere sequences for formation.[65] These pericentromeric chromatin structures, extending outward from each core centromere to a distance of ~25 kb, and heavily decorated with cohesion complexes, may form in order to stably project the core centromere away from its sister chromatid and thereby enhance the efficiency of bipolar attachment of the spindle to the kinetochores of sister chromatids.[31,66–68]

Earlier studies demonstrated that extreme telocentric chromosome fragments showed normal copy number and nondisjunction frequencies, suggestive of normal mitotic chromosome behavior.[69,70] Similarly, recent studies on chromosome fusions by us and by others,[46,64] in which centromeres were positioned in their normal context but at varying positions relative to telomeres, showed very high levels of tolerance to relative position in the chromosome and strict maintenance of euploidy. In this study, we unknowingly challenged the assumption that the minimal *CEN* was sufficient for function, no matter its position on the chromosome, aware of one case in which a "neocentromere" had been recently and successfully created by transplantation within our lab.[3] We thus assumed that transplanting a minimal centromere to any position in the chromosome would lead to a normally functioning mitotic chromosome. We quickly disproved this hypothesis by attempting transplantation of *CEN8*.

On synthetic and wild-type chromosome *VIII*, *CDEI* is attached to the right arm of the chromosome, and *CDEIII* is attached to the left arm, creating a native context that can be visualized as *CDEIII-CDEII-CDEI*. After attempting an initial transplantation with minimal *CEN8* spanning only from *CDEIII to CDEI*, we recovered strains that indeed incorporated the transplanted centromere in two new contexts, but the colonies that passed initial PCR screens contained unexpected yet informative structural variations. In the case of the right arm telocentric transplantation (neocentromere at 523 kb), the surviving structural variant was a partial isochromosome that retained the *CDEIII*-proximal pericentromeric sequence adjacent to the neocentromere. The strain containing this isochromosome was euploid, indicating full mitotic neocentromere function. We discuss the other structural variant from metacentric transplantation below. Hypothesizing that these locations could be inhospitable for centromere function, two additional locations were chosen for transplantation. In several cases of "proximal" transplantation very close to the original centromere position (123 kb), success was achieved with exactly the right neocentromere configuration—deletion of the native *CEN8* and integration into the new site. However, analysis of several strains of this type showed a

substantial level of aneuploidy, nearing a stable disomic state. Similar results were obtained from clones characterized after multiple attempts to transplant near the left telomere. Collectively, these results were consistent with the hypothesis that minimal *CEN8* was in fact not readily transplantable, and it might be missing some sequences required for full function. Similarly, transplantation of minimal *CEN1* into a fusion chromosome led to aneuploidy with the neocentromere. Why some target locations for neocentromeres lead to only rare cases of structural variants that display monosomy and others lead to stable mixed populations of disomic and monosomic cells is not clear, but it suggests the hypothesis that some locations represent sequence contexts that are particularly inhospitable to function of a minimal centromere and others that are only mildly inhospitable and lead to a high rate of nondisjunction and disomy, reflecting partial function of the minimal centromere in this context.

A stable physically dicentric chromosome with one inactive centromere

In the case of the metacentric transplantation, we obtained a single clone representing a truly remarkable structural variant that provides a strong orthogonal datum supporting the hypothesis that minimal *CEN8* lacks some crucial sequence required for "portable" function. This structural variant indeed had the structure we sought, namely a precisely transplanted *CEN8* inserted 98 kb to the "right" of the native *CEN* location, at 203 kb. However, unexpectedly, it retained *CEN8* at the native location and contained a large inversion of the sequences between the two centromeres. Since a plethora of previous studies in *S. cerevisiae* and other species had shown that dicentric chromosomes are unstable and lead to chromosome breakage and breakage fusion bridge cycles, we were initially skeptical of this observation.[71–74] However, multiple rounds of WGS and Hi-C confirmed the structure of the physically dicentric chromosome. We then hypothesized that one of the two centromeres was functionally inactive. We performed experiments to replace each centromere with *URA3* and observed that whereas fast growing Ura⁺ colonies were readily obtained when knocking out the transplanted centromere, no such Ura⁺ colonies were observed when knocking out the native *CEN8*. This experiment provides strong presumptive evidence that the transplanted centromere is nonfunctional (because it can be readily deleted). Tellingly, in this context, as in the case of successfully transplanted but "proximal" aneuploid strain at 123 kb, the transplanted centromere is missing *CDEIII*-flanking pericentromeric sequences, whereas in the isochromosome, which displays full function (i.e., euploidy) in the transplanted state, the *CDEIII*-flanking pericentromere sequences are preserved. We thus hypothesized that this specific pericentromeric sequence might be required for full successful "portable" mitotic centromere function.

Short pericentromeric sequences are required for transplantable *CEN8* function

We deployed a centromeric minichromosome system developed to help study centromere function.[34] In this plasmid/minichromosome, the centromere is included in the context of a much larger portion of *chrVIII* (5 kb) that encompasses both peri-

centromeres. Furthermore, because this plasmid includes the selectable marker *ADE3*, which leads to the formation of white colonies upon plasmid loss in a suitably constructed host strain, it provides a striking visual assay for centromere function/chromosome nondisjunction. We used this system to explicitly investigate whether pericentromeric sequences were required for *CEN8* function by deleting them from the plasmid. These studies clearly implicated the *CDEIII*-proximal pericentromeric sequences as crucial for function. While the minimal core centromere did show some function, it was dramatically impaired relative to the 5-kb extended centromeric region present in the original plasmid. Whereas inclusion of the *CDEI*-proximal pericentromere had little to no effect on plasmid stability, *CDEIII*-proximal pericentromeric DNA rescued plasmid instability. These specific *CDEIII*-flanking sequences appear to improve chromosomal stability since the incidence of chromosome *VIII* aneuploidy was dramatically reduced in additional SSICT experiments containing the expanded *CEN8* sequence.

Limitations of the study

SynVIII is but one of 16 yeast synthetic chromosomes, and the fact that it functions in the context of 15 native chromosomes does not guarantee good function in the context of the rest of the synthetic chromosomes. Our studies point to a requirement for pericentromeric sequences adjacent to the *CDEIII* element of *CEN8*, which seem to be required for function in certain ectopic contexts. The exact nature of these sequences remains to be determined as we did not investigate the specific sequences required here. Furthermore, our findings imply that the other centromeres will have similar but perhaps idiosyncratic requirements for ectopic function if they are to be deployed as "designer neocentromeres." While we saw a similar effect in moving *CEN1* to an ectopic position, suggesting that incomplete centromere function may be a feature of all the yeast minimal centromeres, we cannot say for certain that all 16 minimal centromeres depend on flanking pericentromeric sequences for full function, as defined by transplantability.

CONSORTIA

This work is part of the international Synthetic Yeast Genome (Sc2.0) consortium. The chromosome design and building consortium includes research groups worldwide: Boeke Lab at Johns Hopkins University and New York University (led chromosomes I, III, IV, VI, VIII, IX), Chandrasegaran lab at Johns Hopkins (led chromosomes III and IX), Cai Lab at University of Edinburgh and University of Manchester (led chromosomes II, VII, and tRNA neochromosome), Yue Shen's team at BGI-Research SHENZHEN (led chromosomes II, VII, XIII), Y.J. Yuan's team at Tianjin University (led chromosomes V, X), Dai Lab at Tsinghua University and Shenzhen Institute of Advanced Technology, CAS (led chromosome XII), Ellis Lab at Imperial College London (led chromosome XI), Sakkie Pretorius's team at Macquarie University (led chromosomes XIV, XVI), Matthew Wook Chang's team at National University of Singapore (led chromosome XV), Bader and Boeke Labs at Johns Hopkins University (led design and workflow), and Build-A-Genome undergraduate teams at Johns Hopkins University and Loyola University Maryland (contributed

CellPress
OPEN ACCESS

to chromosomes I, III, IV, VIII, IX). The Sc2.0 consortium includes numerous other participants and are acknowledged on the project web site www.syntheticyeast.org.

STAR★METHODS

Detailed methods are provided in the online version of this paper and include the following:

- KEY RESOURCES TABLE
- RESOURCE AVAILABILITY
  - Lead contact
  - Materials availability
  - Data and code availability
- EXPERIMENTAL MODEL AND SUBJECT DETAILS
  - Yeast strains
  - Bacterial strains
- METHOD DETAILS
  - Synthetic chromosome assembly
  - Meiotic recombination-mediated assembly
  - Synthetic strain modifications via CRISPR
  - Whole genome sequencing
  - Genome sequencing analysis
  - RNA extraction and transcript profiling
  - Sporulation and tetrad dissection
  - Hi-C library preparation
  - Hi-C data processing
  - Centromere transplantation by SSICT
  - Destabilization of aneuploid chromosomes
  - Minichromosome construction and stability assay
- QUANTIFICATION AND STATISTICAL ANALYSIS

SUPPLEMENTAL INFORMATION

Supplemental information can be found online at https://doi.org/10.1016/j.xgen.2023.100437.

AUTHOR CONTRIBUTIONS

J.D.B., S.L., and J.L. conceptualized the study. J.D.B., G.S., and J.S.B. supervised the study. S.L., J.L., L.L.-S., Y.Z., W.Z., M.A.B.H., L.H.M., and F.Y. performed the experiments, including synthetic DNA assembly, construction and analysis of intermediate *synVIII* strains, centromere transplantation, Hi-C library construction and data processing, and RNA sequencing and analysis. S.L.L., N.E., V.F., and E.L. performed whole-genome sequencing and analysis. Build-A-Genome class students contributed building block and minichunk DNA assembly. J.C. and J.S.B. curated the *synVIII* sequencing datasets. The manuscript was drafted by S.L., J.L., L.L.-S., and J.D.B. and edited by all authors.

REFERENCES

1. Zhao, Y., Coelho, C., Hughes, A.L., Lazar-Stefanita, L., Yang, S., Brooks, A.N., Walker, R.S.K., Zhang, W., Lauer, S., Hernandez, C., et al. (2023). Debugging and consolidating multiple synthetic chromosomes reveals combinatorial genetic interactions. Cell. https://doi.org/10.1101/2022.04.11.486913.

2. Luo, J. (2023). Synthetic chromosome fusion: effects on mitotic and meiotic genome structure and function. Cell Genomics.

3. Zhang, W., Lazar-Stefanita, L., Yamashita, H., Shen, M.J., Mitchell, L.A., Kurasawa, H., Haase, M.A.B., Sun, X., Jiang, Q., Lauer, S.L., et al. (2022). Manipulating the 3D organization of the largest synthetic yeast chromosome. Preprint at bioRxiv. https://doi.org/10.1101/2022.04.09.487066.

4. Shen, Y. (2023). Dissecting aneuploidy phenotypes by constructing Sc2.0 chromosome VII and SCRaMbLEing synthetic disomic yeast. Cell Genomics.

5. McCulloch, L.H. (2023). Consequences of a telomerase-related fitness defect and chromosome substitution technology in yeast synIX strains. Cell.

6. Blount, B. (2023). Synthetic yeast chromosome XI design provides a testbed for studying extrachromosomal circular DNA. Cell Genomics.

7. Zhou, C. (2023). Screening and characterization of aging regulators using synthesized yeast chromosome XIII. Cell Genomics.

8. Williams, T. (2023). Parallel laboratory evolution and rational debugging reveal genomic plasticity to Saccharomyces cerevisiae synthetic chromosome XIV defects and rearrangements. Cell Genomics.

9. Foo, J.L. (2023). Establishing Chromosomal Design-Build-Test-Learn through Combinatorial Reconfiguration of a Synthetic Chromosome. Cell Genomics.

10. Goold, H.D. (2023). Construction, debugging and chromosomal stability analysis of a 903kb synthetic Saccharomyces cerevisiae chromosome. Cell Genomics.

11. Schindler, D., Walker, R.S.K., Jiang, S., Brooks, A.N., Wang, Y., Müller, C.A., Cockram, C., Luo, Y., García, A., Schraivogel, D., et al. (2022). Design, Construction, and Functional Characterization of a tRNA Neochromosome in Yeast. Preprint at bioRxiv. https://doi.org/10.1101/2022.10.03.510608.

12. Dymond, J.S., Richardson, S.M., Coombes, C.E., Babatz, T., Muller, H., Annaluru, N., Blake, W.J., Schwerzmann, J.W., Dai, J., Lindstrom, D.L., et al. (2011). Synthetic chromosome arms function in yeast and generate phenotypic diversity by design. Nature *477*, 471–476.

13. Annaluru, N., Muller, H., Mitchell, L.A., Ramalingam, S., Stracquadanio, G., Richardson, S.M., Dymond, J.S., Kuang, Z., Scheifele, L.Z., Cooper, E.M., et al. (2014). Total synthesis of a functional designer eukaryotic chromosome. Science *344*, 55–58.

14. Shen, Y., Wang, Y., Chen, T., Gao, F., Gong, J., Abramczyk, D., Walker, R., Zhao, H., Chen, S., Liu, W., et al. (2017). Deep functional analysis of synII, a

770-kilobase synthetic yeast chromosome. Science *355*, eaaf4791. https://doi.org/10.1126/science.aaf4791.

15. Xie, Z.-X., Li, B.-Z., Mitchell, L.A., Wu, Y., Qi, X., Jin, Z., Jia, B., Wang, X., Zeng, B.-X., Liu, H.-M., et al. (2017). Perfect" designer chromosome V and behavior of a ring derivative. Science *355*, eaaf4704. https://doi.org/10.1126/science.aaf4704.

16. Mitchell, L.A., Wang, A., Stracquadanio, G., Kuang, Z., Wang, X., Yang, K., Richardson, S., Martin, J.A., Zhao, Y., Walker, R., et al. (2017). Synthesis, debugging, and effects of synthetic chromosome consolidation: synVI and beyond. Science *355*, eaaf4831. https://doi.org/10.1126/science.aaf4831.

17. Wu, Y., Li, B.-Z., Zhao, M., Mitchell, L.A., Xie, Z.-X., Lin, Q.-H., Wang, X., Xiao, W.-H., Wang, Y., Zhou, X., et al. (2017). Bug mapping and fitness testing of chemically synthesized chromosome X. Science *355*, eaaf4706. https://doi.org/10.1126/science.aaf4706.

18. Zhang, W., Zhao, G., Luo, Z., Lin, Y., Wang, L., Guo, Y., Wang, A., Jiang, S., Jiang, Q., Gong, J., et al. (2017). Engineering the ribosomal DNA in a megabase synthetic chromosome. Science *355*, eaaf3981. https://doi.org/10.1126/science.aaf3981.

19. Ellis, T. (2019). What is synthetic genomics anyway? Biochemist *41*, 6–9.

20. Zhang, W., Mitchell, L.A., Bader, J.S., and Boeke, J.D. (2020). Synthetic Genomes. Annu. Rev. Biochem. *89*, 77–101.

21. Ostrov, N., Landon, M., Guell, M., Kuznetsov, G., Teramoto, J., Cervantes, N., Zhou, M., Singh, K., Napolitano, M.G., Moosburner, M., et al. (2016). Design, synthesis, and testing toward a 57-codon genome. Science *353*, 819–822.

22. Fredens, J., Wang, K., de la Torre, D., Funke, L.F.H., Robertson, W.E., Christova, Y., Chia, T., Schmied, W.H., Dunkelmann, D.L., Beránek, V., et al. (2019). Total synthesis of Escherichia coli with a recoded genome. Nature *569*, 514–518.

23. Hutchison, C.A., Chuang, R.-Y., Noskov, V.N., Assad-Garcia, N., Deerinck, T.J., Ellisman, M.H., Gill, J., Kannan, K., Karas, B.J., Ma, L., et al. (2016). Design and synthesis of a minimal bacterial genome. Science *351*, aad6253.

24. Venetz, J.E., Del Medico, L., Wölfle, A., Schächle, P., Bucher, Y., Appert, D., Tschan, F., Flores-Tinoco, C.E., van Kooten, M., Guennoun, R., et al. (2019). Chemical synthesis rewriting of a bacterial genome to achieve design flexibility and biological functionality. Proc. Natl. Acad. Sci. USA *116*, 8070–8079.

25. Robertson, W.E., Funke, L.F.H., de la Torre, D., Fredens, J., Elliott, T.S., Spinck, M., Christova, Y., Cervettini, D., Böge, F.L., Liu, K.C., et al. (2021). Sense codon reassignment enables viral resistance and encoded polymer synthesis. Science *372*, 1057–1062.

26. Dymond, J., and Boeke, J. (2012). The Saccharomyces cerevisiae SCRaMbLE system and genome minimization. Bioeng. Bugs *3*, 168–171.

27. Shen, Y., Stracquadanio, G., Wang, Y., Yang, K., Mitchell, L.A., Xue, Y., Cai, Y., Chen, T., Dymond, J.S., Kang, K., et al. (2016). SCRaMbLE generates designed combinatorial stochastic diversity in synthetic chromosomes. Genome Res. *26*, 36–49.

28. Lazar-Stefanita, L., Luo, J., Haase, M.A.B., Zhang, W., and Boeke, J.D. (2022). Stable twin rDNA loci form a single nucleolus in brewer's yeast. bioRxiv. https://doi.org/10.1101/2022.06.14.496147.

29. Fitzgerald-Hayes, M., Clarke, L., and Carbon, J. (1982). Nucleotide sequence comparisons and functional analysis of yeast centromere DNAs. Cell *29*, 235–244.

30. Paldi, F., Alver, B., Robertson, D., Schalbetter, S.A., Kerr, A., Kelly, D.A., Baxter, J., Neale, M.J., and Marston, A.L. (2020). Convergent genes shape budding yeast pericentromeres. Nature *582*, 119–123.

31. Yeh, E., Haase, J., Paliulis, L.V., Joglekar, A., Bond, L., Bouck, D., Salmon, E.D., and Bloom, K.S. (2008). Pericentric chromatin is organized into an intramolecular loop in mitosis. Curr. Biol. *18*, 81–90.

32. Lawrimore, J., and Bloom, K. (2022). Shaping centromeres to resist mitotic spindle forces. J. Cell Sci. *135*, jcs259532. https://doi.org/10.1242/jcs.259532.

33. Ohkuni, K., and Kitagawa, K. (2011). Endogenous transcription at the centromere facilitates centromere activity in budding yeast. Curr. Biol. *21*, 1695–1703.

34. Ling, Y.H., and Yuen, K.W.Y. (2019). Point centromere activity requires an optimal level of centromeric noncoding RNA. Proc. Natl. Acad. Sci. USA *116*, 6270–6279.

35. Hedouin, S., Logsdon, G.A., Underwood, J.G., and Biggins, S. (2022). A transcriptional roadblock protects yeast centromeres. Nucleic Acids Res. *50*, 7801–7815. https://doi.org/10.1093/nar/gkac117.

36. Surosky, R.T., and Tye, B.K. (1985). Construction of telocentric chromosomes in Saccharomyces cerevisiae. Proc. Natl. Acad. Sci. USA *82*, 2106–2110.

37. Lambie, E.J., and Roeder, G.S. (1986). Repression of meiotic crossing over by a centromere (CEN3) in Saccharomyces cerevisiae. Genetics *114*, 769–789.

38. Cottarel, G., Shero, J.H., Hieter, P., and Hegemann, J.H. (1989). A 125 bp CEN6 DNA fragment is sufficient for complete meiotic and mitotic centromere functions in Saccharomyces cerevisiae. Trends Genet. *5*, 322–324. https://doi.org/10.1016/0168-9525(89)90119-4.

39. Clarke, L., and Carbon, J. (1983). Genomic substitutions of centromeres in Saccharomyces cerevisiae. Nature *305*, 23–28.

40. Sikorski, R.S., and Hieter, P. (1989). A system of shuttle vectors and yeast host strains designed for efficient manipulation of DNA in Saccharomyces cerevisiae. Genetics *122*, 19–27.

41. Lin, Q., Jia, B., Mitchell, L.A., Luo, J., Yang, K., Zeller, K.I., Zhang, W., Xu, Z., Stracquadanio, G., Bader, J.S., et al. (2015). RADOM, an efficient in vivo method for assembling designed DNA fragments up to 10 kb long in Saccharomyces cerevisiae. ACS Synth. Biol. *4*, 213–220.

42. Richardson, S.M., Mitchell, L.A., Stracquadanio, G., Yang, K., Dymond, J.S., DiCarlo, J.E., Lee, D., Huang, C.L.V., Chandrasegaran, S., Cai, Y., et al. (2017). Design of a synthetic yeast genome. Science *355*, 1040–1044.

43. Gottschling, D.E., Aparicio, O.M., Billington, B.L., and Zakian, V.A. (1990). Position effect at S. cerevisiae telomeres: reversible repression of Pol II transcription. Cell *63*, 751–762.

44. Shen, M.J., Wu, Y., Yang, K., Li, Y., Xu, H., Zhang, H., Li, B.-Z., Li, X., Xiao, W.-H., Zhou, X., et al. (2018). Heterozygous diploid and interspecies SCRaMbLEing. Nat. Commun. *9*, 1934.

45. Richardson, S.M., Nunley, P.W., Yarrington, R.M., Boeke, J.D., and Bader, J.S. (2010). GeneDesign 3.0 is an updated synthetic biology toolkit. Nucleic Acids Res. *38*, 2603–2606.

46. Luo, J., Sun, X., Cormack, B.P., and Boeke, J.D. (2018). Karyotype engineering by chromosome fusion leads to reproductive isolation in yeast. Nature *560*, 392–396.

47. Hill, A., and Bloom, K. (1987). Genetic manipulation of centromere function. Mol. Cell Biol. *7*, 2397–2405.

48. Reid, R.J.D., Sunjevaric, I., Voth, W.P., Ciccone, S., Du, W., Olsen, A.E., Stillman, D.J., and Rothstein, R. (2008). Chromosome-scale genetic mapping using a set of 16 conditionally stable Saccharomyces cerevisiae chromosomes. Genetics *180*, 1799–1808.

49. Hill, A., and Bloom, K. (1989). Acquisition and processing of a conditional dicentric chromosome in Saccharomyces cerevisiae. Mol. Cell Biol. *9*, 1368–1370.

50. Song, W., Gawel, M., Dominska, M., Greenwell, P.W., Hazkani-Covo, E., Bloom, K., and Petes, T.D. (2013). Nonrandom distribution of interhomolog recombination events induced by breakage of a dicentric chromosome in Saccharomyces cerevisiae. Genetics *194*, 69–80.

51. Cook, D., Long, S., Stanton, J., Cusick, P., Lawrimore, C., Yeh, E., Grant, S., and Bloom, K. (2021). Behavior of dicentric chromosomes in budding yeast. PLoS Genet. *17*, e1009442.

52. Lieberman-Aiden, E., van Berkum, N.L., Williams, L., Imakaev, M., Ragoczy, T., Telling, A., Amit, I., Lajoie, B.R., Sabo, P.J., Dorschner, M.O., et al. (2009). Comprehensive mapping of long-range interactions reveals folding principles of the human genome. Science *326*, 289–293.

53. Koren, A., Soifer, I., and Barkai, N. (2010). MRC1-dependent scaling of the budding yeast DNA replication timing program. Genome Res. *20*, 781–790.

54. Hegemann, J.H., Shero, J.H., Cottarel, G., Philippsen, P., and Hieter, P. (1988). Mutational analysis of centromere DNA from chromosome VI of Saccharomyces cerevisiae. Mol. Cell Biol. *8*, 2523–2535.

55. Hegemann, J.H., and Fleig, U.N. (1993). The centromere of budding yeast. Bioessays *15*, 451–460.

56. Murray, A.W., and Szostak, J.W. (1983). Pedigree analysis of plasmid segregation in yeast. Cell *34*, 961–970.

57. Clarke, L., and Carbon, J. (1980). Isolation of a yeast centromere and construction of functional small circular chromosomes. Nature *287*, 504–509.

58. Karim, A.S., Curran, K.A., and Alper, H.S. (2013). Characterization of plasmid burden and copy number in Saccharomyces cerevisiae for optimization of metabolic engineering applications. FEMS Yeast Res. *13*, 107–116.

59. Fang, F., Salmon, K., Shen, M.W.Y., Aeling, K.A., Ito, E., Irwin, B., Tran, U.P.C., Hatfield, G.W., Da Silva, N.A., and Sandmeyer, S. (2011). A vector set for systematic metabolic engineering in Saccharomyces cerevisiae. Yeast *28*, 123–136.

60. Ryan, O.W., Skerker, J.M., Maurer, M.J., Li, X., Tsai, J.C., Poddar, S., Lee, M.E., DeLoache, W., Dueber, J.E., Arkin, A.P., and Cate, J.H.D. (2014). Selection of chromosomal DNA libraries using a multiplex CRISPR system. Elife *3*, e03703. https://doi.org/10.7554/eLife.03703.

61. Flagg, M.P., Kao, A., and Hampton, R.Y. (2019). Integrating after CEN Excision (ICE) Plasmids: Combining the ease of yeast recombination cloning with the stability of genomic integration. Yeast *36*, 593–605.

62. Bloom, K.S., and Carbon, J. (1982). Yeast centromere DNA is in a unique and highly ordered structure in chromosomes and small circular minichromosomes. Cell *29*, 305–317.

63. Bloom, K.S., Fitzgerald-Hayes, M., and Carbon, J. (1983). Structural analysis and sequence organization of yeast centromeres. Cold Spring Harbor Symp. Quant. Biol. *47 Pt 2*, 1175–1185.

64. Shao, Y., Lu, N., Wu, Z., Cai, C., Wang, S., Zhang, L.-L., Zhou, F., Xiao, S., Liu, L., Zeng, X., et al. (2018). Creating a functional single-chromosome yeast. Nature *560*, 331–335.

65. Lazar-Stefanita, L., Luo, J., Montagne, R., Thierry, A., Sun, X., Mercy, G., Mozziconacci, J., Koszul, R., and Boeke, J.D. (2022). Karyotype engineering reveals spatio-temporal control of replication firing and gene contacts. Cell Genom. *2*, 100163. None.

66. Glynn, E.F., Megee, P.C., Yu, H.-G., Mistrot, C., Unal, E., Koshland, D.E., DeRisi, J.L., and Gerton, J.L. (2004). Genome-Wide Mapping of the Cohesin Complex in the Yeast Saccharomyces cerevisiae. PLoS Biol. *2*, e259. https://doi.org/10.1371/journal.pbio.0020259.

67. Lengronne, A., McIntyre, J., Katou, Y., Kanoh, Y., Hopfner, K.-P., Shirahige, K., and Uhlmann, F. (2006). Establishment of Sister Chromatid Cohesion at the S. cerevisiae Replication Fork. Mol. Cell *23*, 787–799. https://doi.org/10.1016/j.molcel.2006.08.018.

68. Ng, T.M., Waples, W.G., Lavoie, B.D., and Biggins, S. (2009). Pericentromeric sister chromatid cohesion promotes kinetochore biorientation. Mol. Biol. Cell *20*, 3818–3827.

69. Vollrath, D., Davis, R.W., Connelly, C., and Hieter, P. (1988). Physical mapping of large DNA by chromosome fragmentation. Proc. Natl. Acad. Sci. USA *85*, 6027–6031. https://doi.org/10.1073/pnas.85.16.6027.

70. Morrow, D.M., Connelly, C., and Hieter, P. (1997). Break copy" duplication: a model for chromosome fragment formation in Saccharomyces cerevisiae. Genetics *147*, 371–382.

71. McClintock, B. (1941). The Stability of Broken Ends of Chromosomes in Zea Mays. Genetics *26*, 234–282.

72. Mann, C., and Davis, R.W. (1983). Instability of dicentric plasmids in yeast. Proc. Natl. Acad. Sci. USA *80*, 228–232.

73. Haber, J.E., and Thorburn, P.C. (1984). Healing of broken linear dicentric chromosomes in yeast. Genetics *106*, 207–226.

74. Koshland, D., Rutledge, L., Fitzgerald-Hayes, M., and Hartwell, L.H. (1987). A genetic analysis of dicentric minichromosomes in Saccharomyces cerevisiae. Cell *48*, 801–812.

75. Brachmann, C.B., Davies, A., Cost, G.J., Caputo, E., Li, J., Hieter, P., and Boeke, J.D. (1998). Designer deletion strains derived from Saccharomyces cerevisiae S288C: a useful set of strains and plasmids for PCR-mediated gene disruption and other applications. Yeast *14*, 115–132.

76. Xie, Z.-X., Mitchell, L.A., Liu, H.-M., Li, B.-Z., Liu, D., Agmon, N., Wu, Y., Li, X., Zhou, X., Li, B., et al. (2018). Rapid and Efficient CRISPR/Cas9-Based Mating-Type Switching of Saccharomyces cerevisiae. G3 *8*, 173–183.

77. Robinson, J.T., Thorvaldsdóttir, H., Winckler, W., Guttman, M., Lander, E.S., Getz, G., and Mesirov, J.P. (2011). Integrative genomics viewer. Nat. Biotechnol. *29*, 24–26.

78. Bolger, A.M., Lohse, M., and Usadel, B. (2014). Trimmomatic: a flexible trimmer for Illumina sequence data. Bioinformatics *30*, 2114–2120.

79. Langmead, B., and Salzberg, S.L. (2012). Fast gapped-read alignment with Bowtie 2. Nat. Methods *9*, 357–359.

80. Imakaev, M., Fudenberg, G., McCord, R.P., Naumova, N., Goloborodko, A., Lajoie, B.R., Dekker, J., and Mirny, L.A. (2012). Iterative correction of Hi-C data reveals hallmarks of chromosome organization. Nat. Methods *9*, 999–1003.

81. Lesne, A., Riposo, J., Roger, P., Cournac, A., and Mozziconacci, J. (2014). 3D genome reconstruction from chromosomal contacts. Nat. Methods *11*, 1141–1143.

82. Wickham, H. (2016). ggplot2: Elegant Graphics for Data Analysis (Springer-Verlag).

83. Bray, N.L., Pimentel, H., Melsted, P., and Pachter, L. (2016). Erratum: Near-optimal probabilistic RNA-seq quantification. Nat. Biotechnol. *34*, 888.

84. Li, H., Handsaker, B., Wysoker, A., Fennell, T., Ruan, J., Homer, N., Marth, G., Abecasis, G., and Durbin, R.; 1000 Genome Project Data Processing Subgroup (2009). Genome Project Data Processing Subgroup (2009). The Sequence Alignment/Map format and SAMtools. Bioinformatics *25*, 2078–2079.

85. Quinlan, A.R., and Hall, I.M. (2010). BEDTools: a flexible suite of utilities for comparing genomic features. Bioinformatics *26*, 841–842.

86. Pimentel, H., Bray, N.L., Puente, S., Melsted, P., and Pachter, L. (2017). Differential analysis of RNA-seq incorporating quantification uncertainty. Nat. Methods *14*, 687–690.

87. Gietz, R.D., and Schiestl, R.H. (2007). High-efficiency yeast transformation using the LiAc/SS carrier DNA/PEG method. Nat. Protoc. *2*, 31–34.

88. Hanahan, D., Jessee, J., and Bloom, F.R. (1991). Plasmid transformation of Escherichia coli and other bacteria. Methods Enzymol. *204*, 63–113.

89. Garrison, E., and Marth, G. (2012). Haplotype-based variant detection from short-read sequencing. Preprint at arXiv, [q-bio.GN]. https://doi.org/10.48550/arXiv.1207.3907.

90. Cameron, D.L., Baber, J., Shale, C., Valle-Inclan, J.E., Besselink, N., van Hoeck, A., Janssen, R., Cuppen, E., Priestley, P., and Papenfuss, A.T. (2021). GRIDSS2: comprehensive characterisation of somatic structural variation using single breakend variants and structural variant phasing. Genome Biol. *22*, 202.

91. Bray, N.L., Pimentel, H., Melsted, P., and Pachter, L. (2016). Melsted, and Pachter Near-optimal RNA-Seq quantification with kallisto. Nat. Biotechnol. *34*, 888.

92. Deng, C., and Saunders, W.S. (2001). ADY1, A Novel Gene Required for Prospore Membrane Formation at Selected Spindle Poles inSaccharomyces cerevisiae. MBoC *12*, 2646–2659.

93. Belton, J.-M., McCord, R.P., Gibcus, J.H., Naumova, N., Zhan, Y., and Dekker, J. (2012). Hi-C: a comprehensive technique to capture the conformation of genomes. Methods *58*, 268–276.

94. Lazar-Stefanita, L., Scolari, V.F., Mercy, G., Muller, H., Guérin, T.M., Thierry, A., Mozziconacci, J., and Koszul, R. (2017). Cohesins and condensins orchestrate the 4D dynamics of yeast chromosomes during the cell cycle. EMBO J. *36*, 2684–2697.

95. Cournac, A., Marie-Nelly, H., Marbouty, M., Koszul, R., and Mozziconacci, J. (2012). Normalization of a chromosomal contact map. BMC Genom. *13*, 436.

96. Li, H., Wysoker, F., and Ruan The Sequence alignment/map (SAM) format and SAMtools. Bioinformatics.

STAR★METHODS

KEY RESOURCES TABLE

REAGENT or RESOURCE	SOURCE	IDENTIFIER
Bacterial and viral strains		
TOP10 *E. coli* strain	Jef Boeke's laboratory	N/A
Chemicals, peptides, and recombinant proteins		
Zymolyase 100T	US Biological	Cat#Z1004
Lithium acetate dihydrate	Sigma-Aldrich	Cat#L6883
Polyethylene glycol (PEG)	Sigma-Aldrich	Cat#81188
Herring sperm DNA	Promega	Cat#D1816
Potassium acetate	Fisher	Cat#BP364
Zinc acetate dihydrate	Sigma-Aldrich	Cat#Z0625
(S)-(+)-Camptothecin	Sigma-Aldrich	Cat#C9911
D-Sorbitol	Sigma-Aldrich	Cat#S1876
6-Azauracil	Sigma-Aldrich	Cat#A1757
Hydroxyurea	Sigma-Aldrich	Cat#H8627
Methyl methanesulfonate	Sigma-Aldrich	Cat#129925
Methyl 1-(butylcarbamoyl)-2-benzimidazolecarbamate (Benomyl)	Sigma-Aldrich	Cat#381586
Cycloheximide	Sigma-Aldrich	Cat#01810
GoTaq Green Master Mix	Promega	Cat#M7123
Phusion Hot Start Flex 2X Master Mix	Thermo Fisher Scientific	Cat#M0536
RNase A	Thermo Fisher Scientific	Cat#EN0531
Formaldehyde solution	Sigma-Aldrich	Cat#F8775
MboI	NEB	Cat#R0147
Biotin-14-dCTP	Invitrogen	Cat#19518018
Klenow enzyme	NEB	Cat#M0210L
T4 DNA ligase	Thermo Scientific	Cat#EL0014
Proteinase K	Thermo Scientific	Cat#EO0491
Invitrogen™ Dynabeads™ MyOne™ Streptavidin C1	Invitrogen	Cat#65001
KAPA-HiFi	Kapa Biosystems	Cat#KK2602
Critical commercial assays		
Zyppy Plasmid Miniprep Kit	Zymo Research	Cat#D4037
Fungi/Yeast Genomic DNA Isolation Kit	Norgen	Cat#27300
Qubit dsDNA HS Assay Kit	Thermo Fisher Scientific	Cat#Q32854
NEBNext Ultra II FS DNA Library Kit	NEB	Cat#E7805
Zymoclean™ Large Fragment DNA Recovery	Zymo Research	Cat#D4046
RNeasy Mini Kit	QIAGEN	Cat#74106
NEBNext Ultra II RNA Library Prep Kit	NEB	Cat#E7770
Qubit RNA BR Assay Kit	Thermo Fisher Scientific	Cat#Q10210
NextSeq 500/550 High Output Kit v2.5 (75 Cycles)	Illumina	Cat#20024906
NextSeq 500/550 High Output Kit v2.5 (150 Cycles)	Illumina	Cat#20024907
Deposited data		
Genome sequencing data	This study	N/A

(Continued on next page)

Continued

REAGENT or RESOURCE	SOURCE	IDENTIFIER
RNA-seq data	This study	N/A
Hi-C data	This study	N/A
Plasmid sequence files	This study	N/A
Experimental models: Organisms/strains		
Saccharomyces cerevisiae: BY4741	Brachman et al.[75]	N/A
All other strains used in this study are listed in Tables S2, S5, S6, and S8	N/A	N/A
Oligonucleotides		
Primers and gRNA sequences are listed in Table S9	N/A	N/A
Recombinant DNA		
Plasmid: pNA0306 (SpCas9 with TEF1 promoter and CYC1 terminator in pRS415 backbone)	Xie et al.[76]	Addgene Plasmid #169452
Plasmid: pNA0519 (SpCas9 with TEF1 promoter and CYC1 terminator in pRS413 backbone)	Jef Boeke's laboratory	N/A
Plasmid: pNA0304 (contains gRNA assembled using Gibson)	Jef Boeke's laboratory	N/A
Plasmid: pNA0308 (contains up to two gRNAs assembled using Gibson)	Jef Boeke's laboratory	N/A
Plasmid: pNA0525 (contains gRNA assembled using Gibson)	Jef Boeke's laboratory	N/A
Plasmid: bJL179	Luo et al.[46]	N/A
Plasmid: WYYp299	Ling and Yuen[34]	N/A
Plasmid: bSLL49	This study	N/A
Plasmid: bSLL50	This study	N/A
Plasmid: bSLL52	This study	N/A
Plasmid: bSLL55	This study	N/A
Software and algorithms		
R	R Core Team	https://www.R-project.org/
Rstudio v1.3.1093	Rstudio	https://www.rstudio.com
SYSeq	Unpublished data	N/A
Integrated Genomics Viewer (IGV) v2.7.2	Broad Institute[77]	http://software.broadinstitute.org/software/igv/
Trimmomatic v0.39	Bolger, Lohse, and Usadel[78]	http://www.usadellab.org/cms/index.php?page=trimmomatic
Bowtie 2 v2.2.9	Langmead and Salzberg[79]	http://bowtie-bio.sourceforge.net/bowtie2/index.shtml
HICLib	Imakaev et al.[80]	N/A
ShRec3d	Lesne et al.[81]	N/A
PyMol	Molecular Graphics System, Version 2.0 Schrodinger, LLC	N/A
ggplot2 v3.3.5	Wickham et al.[82]	https://ggplot2.tidyverse.org/
Kallisto v0.46.0	Bray et al.[83]	https://pachterlab.github.io/kallisto/
SAMtools v1.9	Li et al.[84]	http://samtools.sourceforge.net/
BEDtools v2.26.0	Quinlan and Hall[85]	https://github.com/arq5x/bedtools2/
sleuth v0.30.0	Pimentel et al.[86]	https://pachterlab.github.io/sleuth/
Other		
Resource website for Sc2.0	N/A	https://syntheticyeast.github.io/

RESOURCE AVAILABILITY

Lead contact

Further information should be directed to and will be fulfilled by the lead contact, Jef D. Boeke (jef.boeke@nyulangone.org).

Materials availability

All unique/stable reagents generated in this study are available from the lead contact upon reasonable request.

Data and code availability

- Data: All data are available under the overarching Sc2.0 umbrella BioProject PRJNA351844. The data for *synVIII* are provided under Bioproject PRJNA851090. The specific data reported here were deposited to GenBank accession number CP134974 for the synVIII sequence and Gene Expression Omnibus subseries GSE244852 for Hi_C and subseries GSE244513 for RNA-seq. Original source data for Figure 5 is available in Table S7.
- Code: This work did not generate any new code.
- Any additional information required to reanalyze the data reported in this paper is available from the lead contact upon request.

EXPERIMENTAL MODEL AND SUBJECT DETAILS

Yeast strains

All yeast strains used in this study were derived from BY4741. Key versions of *synVIII* are listed in Table S2. Intermediate strain names, genotypes, and synthetic chromosome version numbers for *synVIII* assembly are provided in Table S8. Yeast strains generated via SSICT are described in Table S5 and Table S6. All yeast transformations were performed using standard lithium acetate and PEG protocols.[87] Herring sperm was used as a carrier for transformed DNA. Strains were cultured in a variety of media conditions including yeast extract with peptone and 2% dextrose (YPD), yeast extract with peptone and 3% glycerol (YPG) and synthetic complete media (SC). YPD, YPG, and SC were prepared following standard recipes. SC plates lacking specific nutrients were often used for selection. For example, SC–Ura plates do not contain uracil. Additional media types for growth assays (Figure S6) were prepared and include the following plate types: pH 4 and pH 8: pH of 2X YEP + dextrose adjusted using HCl and NaOH, respectively before adding agar; camptothecin (Sigma-Aldrich, C9911): 0.1 μg/mL, 0.5 μg/mL, or 1.0 μg/mL in YPD; sorbitol (Sigma-Aldrich, S1876): 0.5 M, 1.0 M, 1.5 M, or 2.0 M in YPD; 6-azauracil (Sigma-Aldrich, A1757): 100 μg/mL in SC medium; hydroxyurea (Sigma-Aldrich, H8627): 0.2M in YPD; MMS: methyl methanesulfonate (Sigma-Aldrich, 129925), 0.05% in YPD; benomyl (Sigma-Aldrich, 381586): 15 μg/mL in YPD; cycloheximide (Sigma-Aldrich, 01810): 10 μg/mL in YPD liquid medium for 2 h followed by plating to YPD; H_2O_2 (Millipore, 88597): 1 mM in YPD liquid medium for 2 h followed by plating to YPD.

Bacterial strains

All bacterial strains used in this study were derived from *E. coli* TOP10 cells originally obtained from Invitrogen. TOP10 cells were made chemically competent using standard protocols.[88] Strains were cultured in Luria Broth (LB) or on LB agar plates with the appropriate antibiotics (carbenicillin or kanamycin) added to maintain plasmids. Plasmids were isolated from *E. coli* cells using the Zyppy Plasmid Miniprep Kit (Zymo Research, D4037). All CRISPR/Cas9 experiments were performed with human-optimized *S. pyogenes* Cas9 (using the *TEF1* promoter) cloned into plasmids pNA0306 and pNA0519. Single-guide RNAs were assembled into plasmids pNA0304, pNA0308, and pNA0525.

METHOD DETAILS

Synthetic chromosome assembly

BioStudio was used to design *synVIII*, following the same principles as all other Sc2.0 chromosomes (Figure S1). A bottom-up strategy was used to assemble *synVIII*. Overlapping 60–79 bp oligos were assembled into ~750 bp building blocks, which were further assembled into 2–4 kb minichunks.[13] Next, ~10 kb chunks were synthesized through homologous recombination of minichunks in yeast.[41] Five chunks were digested with specific restriction enzymes and ligated to form megachunk A before integrating into the native yeast genome as previously described.[16] For megachunks B, C, D, H and N, minichunks were integrated directly (i.e., they were not assembled into chunks first). For all remaining megachunks, a mix of minichunks and chunks were used for genome integration. Details are included in Table S1. All the intermediate materials (building blocks, minichunks and chunks) were sequence-verified before moving to the next stage of assembly. After each round of megachunk integration, wild-type and synthetic PCR tags were used to screen for candidates with all designed synthetic DNA integrations. Wild type yeast and pooling of chunks and/or minichunks served as negative control and positive control for the PCR tags validation, respectively.

Meiotic recombination-mediated assembly

The replacement of wild-type DNA to synthetic DNA was performed in parallel in three haploid yeast strains as schematized in Figure S2: (yJL278) *MATa*, containing megachunks A to D and *URA3*; (yJL191) *MATalpha*, containing megachunks D to I and *LEU2*; and (yJL220) *MATa*, containing megachunks G to L and *URA3*. Strain yJL191 was subsequently mated to strain yJL220 and sporulated to generate strain yJL231 (*MATalpha*, containing megachunks D to L and *URA3*). Megachunks M and N were consecutively integrated into strain yJL231 through the traditional *LEU2-URA3* SwAP-In method to generate the strain yJL267 (*MATalpha*) carrying megachunk D to megachunk N. Strain yJL267 was back-crossed with yJL220 to generate yJL306 (*MATalpha*, with megachunks D to

N) to remove a small duplication. Strain yJL278 (*MATa*, containing megachunks A to D and *URA3*) was crossed with another intermediate strain yJL179 (*MAT*alpha, carrying megachunks D to G and *LEU2*) to generate strain yWZ084 (*MATa*, containing megachunks A to G and *LEU2*). The final strain was generated from a cross between strain yJL306 and strain yWZ084.

Synthetic strain modifications via CRISPR

After completion of an initial draft *synVIII* strain, CRISPR-Cas9 mediated yeast transformations were used to integrate 25 kb of missing synthetic sequences in megachunk C, repair a 30 kb duplication in megachunk G, and modify the original *synVIII* design in accordance with an updated version of the *S. cerevisiae* reference genome. Several stop codon swaps were also performed using CRISPR-Cas9. Donor DNA was amplified using PCR with Phusion Hot Start Flex 2X Master Mix (Thermo Scientific, M0536). All edits were verified by colony PCR screening using GoTaq Green (Promega, M7123), Sanger sequencing (Genewiz), and WGS as described below. Single guide RNAs (sgRNAs) and primers used are described in Table S9.

Whole genome sequencing

Genomic DNA was extracted from cell pellets using a Fungi/Yeast Genomic DNA Isolation Kit (Norgen, 27300) and RNAse A (Thermo Fisher Scientific, EN0531). Genomic DNA was quantified with a Qubit dsDNA HS Assay (Thermo Fisher Scientific, Q32854). Whole genome sequencing (WGS) libraries were prepared using the NEBNext Ultra II FS DNA library prep kit (NEB E7805) with at least 100 ng of genomic DNA as input. Libraries were quantified by Qubit and pooled by balancing their final concentrations. Pooled libraries were sequenced using an Illumina NextSeq 500 and paired-end protocols of 36,36 or 75,75 (Illumina 20024906, Illumina 20024907).

Genome sequencing analysis

Illumina paired-end reads were analyzed using the Synthetic Yeast sequencing (SYseq) pipeline (Stracquadanio, G. et al., in preparation). Reads were preprocessed to remove adapters and bases with low quality scores and aligned to a BY4741 reference genome in which native chromosome *VIII* is replaced by the *synVIII* reference designed in BioStudio. Single nucleotide variants (SNVs) and short indels were identified using a freebayes protocol.[89] Structural variants (SVs) and copy number variants (CNVs) were detected by combining GRIDSS[90] with a new copy number calling algorithm designed specifically for haploid strains. Results were organized into VCF and bigWig files for analysis and visualization, with a browser-based platform available for straightforward variant reporting.

RNA extraction and transcript profiling

For transcript profiling, total RNA was isolated from 3 biological replicates of the *synVIII* strain ySLL185. Single yeast colonies were inoculated in 3 mL of YPD at 30°C with rotation overnight, then diluted to $A_{600} = 0.1$ in 5 mL of fresh YPD medium. Cells were harvested after reaching $A_{600} = 0.8–1.0$. Total RNA was extracted using the RNeasy extraction kit (Qiagen, 74106), quantified using the Qubit RNA BR Assay Kit (Thermo Fisher Scientific, Q10210), and then 1 μg of total RNA was used as input for RNA library preparation (NEB E7770).

Libraries were sequenced using an Illumina NextSeq 500 with a paired-end 36,36 protocol (Illumina 20024906). Reads were processed using Trimmomatic to remove Illumina barcodes and adapter sequences, then aligned to the S288C reference with Kallisto.[78,91] Analysis was performed using the Sleuth package in R.[86] Log2 fold change values were calculated and tested for significance with Wald's test using an adjusted p value with corrections for multiple hypothesis testing (Benjamini-Hochberg method).

Certain genes showed statistically significant differences between the WT and *synVIII* strains. *FLO5* is a ''repeat-smashed'' gene that has been synonymously recoded by design, with only 72% identity to the wild-type sequence. As a result, synthetic *FLO5* aligns poorly to the reference and appears down-regulated when compared to BY4741. *PFS1* encodes a sporulation protein required for prospore membrane formation[92] and has low expression levels in rich medium, suggesting its down-regulation may be an artifact. Consistent with this idea, *synVIII* homozygous diploids are capable of sporulation (Figure 2F). The only significantly up-regulated gene on *synVIII* is *YHR073W-A*, a small dubious open reading frame unlikely to encode a functional protein. *YHR073W-A* itself contains no synthetic features but is located within the gene *OSH3*, which is not differentially expressed according to these data. Of three genes located on other chromosomes that are differentially expressed, two are retrotransposon *Gag/Pol* genes.

Sporulation and tetrad dissection

Sporulation medium was prepared using a 50x base consisting of 50 g potassium acetate (Fisher, BP364) and 0.25 g zinc acetate dihydrate (Sigma-Aldrich, Z0625) in 100 mL H₂O. Final 1x sporulation media was prepared from 2 mL of 50x sporulation medium base plus 300 μL of 10% yeast extract, 200 μM uracil, 2 mM leucine 300 μM histidine, and H₂O to 100 mL. To prepare strains for sporulation, a single colony of each strain was inoculated into 5 mL YPD and incubated at 30°C overnight with rotation. Overnight cultures were diluted to an OD of ~1 in YPD and grown to an OD of ~4, washed five times with water, and resuspended in 2 mL of 1X sporulation medium. Strains were incubated at room temperature for 7–10 days with rotation, and monitored for the presence of tetrads. For tetrad dissection, 100 μL of these resuspended yeast cells in sporulation medium were washed and incubated with

25 μL of 0.5 mg/mL zymolyase in 1M sorbitol for 8 min 200 μL of 1M sorbitol was added to the cells, and 10 μL of the resulting mixture was added to a YPD plate. Tetrads were separated and picked using a dissection microscope (Singer Instruments). Spores were grown for 2–3 days on YPD until visible colonies emerged.

Hi-C library preparation

Hi-C experiments and data analysis were performed as described[28,93,94] unless otherwise specified in the following method. Briefly, three independent colonies of ySLL223 were inoculated into 5 mL YPD medium and grown overnight at 30°C. The following day 10^9 cells (approximately 80–100 OD) were subcultured into 100 mL YPD for 3 h of growth at 30°C. Cells were crosslinked by 3% [v/v] formaldehyde (Sigma-Aldrich, F8775) for 20 min at room temperature and subsequently quenched with glycine 350 mM for 15 min at 4°C in mild agitation. Crosslinked cells were harvested and suspended in 10 mL spheroplast solution (1M sorbitol, 50 mM potassium phosphate, 5 mM DTT, 250 U zymolyase 100T (US Biological, Z1004)) for 50 min incubation at 30°C. Spheroplasts were washed with 10 mL of cold 1M sorbitol and resuspended in 2 mL of 0.5% SDS at 65°C for 20 min 125 U of *MboI* (NEB, R0147) were used for overnight digestion (16 h) of the genomic DNA from fixed yeast cells resuspended in 3 mL final volume (1x Cutsmart NEBuffer, 0.33% SDS and 2% Triton) at 37°C. The digestion product was centrifuged at 18000xg for 20 min and the pellet was subsequently suspended in 200 μL cold water. DNA sticky ends were filled with biotin-14-dCTP (Invitrogen, 19518018) by Klenow enzyme (NEB, M0210L) at 37°C for 80 min. Biotinylated DNA was ligated with 60 U T4 DNA ligase (Thermo Scientific, EL0014) in 1.2 mL final volume at room temperature for 2 h in mild agitation. Ligation product was reverse cross-linked by 0.5 mg/mL proteinase K (Thermo Scientific, EO0491) in 0.5% SDS, 25 mM EDTA buffer at 65°C for 4 h. The reverse cross linked sample was ethanol precipitated and purified using the large fragment DNA recovery kit (Zymo Research, D4046). Religated-biotinylated restriction fragments were pulled down using Dynabeads MyOne Streptavidin C1 magnetic beads (Invitrogen 65001) according to the manufacture protocol. The purified Hi-C library was used as input material for the NEBNext Ultra II FS DNA library prep kit (NEB, E7805) with 6-cycle PCR amplification using KAPA-HiFi (Kapa Biosystems, KK2602). The DNA library was sequenced using an Illumina NextSeq 500 75-cycle high output kit (Illumina 20024906).

Hi-C data processing

To generate contact maps: paired-end reads were processed using the HICLib algorithm[80] adapted for the *S. cerevisiae* genome. Read-pairs were independently mapped using Bowtie 2[79] (mode: –very-sensitive –rdg 500,3 –rfg 500,3) on the corresponding reference sequence (S288c and accordingly modified versions of it) indexed for the *MboI* restriction site. In the contact frequency maps, the unwanted restriction fragments (RFs) were filtered out (e.g., loops, non-digested fragments, etc.; for details see,[95] whereas, the valid RFs were binned into units of fixed size bins of 5 kb. Bins with a high variance in contact frequency (<1.5 S. D. or 1.5–2 S.D.) were discarded to remove potential biases resulting from the uneven distribution of restriction sites and variation in GC% and mappability. Note that in the case of *CEN8* sequence duplication, at native (n*CEN8*) and ectopic (e*CEN8*) locations (as described in Figure 4), the bins containing the centromere sequences were filtered out as they would be ambiguously mapped. The filtered contact maps were normalized using the sequential component normalization procedure (SCN) REF Cournac et al. 2012. Approximately 10 million valid contacts were used to generate a genomic contact map for each technical triplicate. For the 3D representations we used the "Shortest-path Reconstruction in 3D" (ShRec3d) algorithm,[81] with the exact specifications described by.[65] Finally, the average genome structures were visualized using PyMol (Molecular Graphics System, Version 2.0 Schrodinger, LLC).

Centromere transplantation by SSICT

CEN8 transplantations were performed with CRISPR using pre-transformed spCa9 in BY4741 and the *synVIII* strain ySLL217. In each experiment, 1–2 plasmids harboring 2–3 different sgRNAs and 2 different donor DNAs were transformed simultaneously in a single step. A previously designed sgRNA plasmid bJL179 was used to target native *CEN8* (n*CEN8*).[46] This plasmid was modified by Gibson assembly to include additional sgRNAs for targeting various ectopic (e*CEN8*) sites. For some experiments, additional sgRNA plasmids SLL236 or SLL237 were used in combination with modified bJL179. 50 ng of each sgRNA plasmid was transformed. Donor DNA used to delete n*CEN8* was designed previously,[46] while donor DNA for integrating e*CEN8* was generated using fusion PCR from primers listed in Table S9. Donor DNA was amplified using PCR with Phusion Hot Start Flex 2X Master Mix (Thermo Scientific, M0536). At least 400 ng of donor DNAs were transformed in each experiment. CRISPR candidates were selected on SC media containing the appropriate nutrient dropouts. Successful transplantations were identified by colony PCR screening using GoTaq Green (Promega, M7123), Sanger sequencing (Genewiz), and WGS as described above. Chromosome copy numbers were quantified relative to whole genome coverage after generating pileup files (i.e., reads per base pair) using SamTools.[96] Strains generated via SSICT are listed in Table S5 and Table S6.

Destabilization of aneuploid chromosomes

We attempted to selectively destabilize aneuploid chromosomes resulting from SSICT using three different approaches. First, we integrated a destabilizing cassette consisting of a *URA3* gene and the GAL promoter adjacent to *CEN8* on one copy of *chrVIII*.[48] PCR primers oSLL244-247 and Phusion Hot Start Flex 2X Master Mix (Thermo Scientific, M0536) were used to amplify the pGAL-*CEN8* donor from bLM185, which was subsequently integrated using yeast transformation with low concentrations of donor DNA (~200 ng total). Colony PCR screening using GoTaq Green (Promega, M7123) with primers oSLL231, oSLL234, oYZ270,

and oYZ600 was used to confirm heterozygous integration of the donor DNA. Heterozygous colonies underwent galactose induction followed by 5-FOA selection,[48] and then PCR-screened candidates were prepared for WGS. In the second approach, we devised a novel strategy to replace the gene *ARG4* with *URA3* on one copy of *chrVIII*. PCR primers oSLL265-267 and Phusion Hot Start Flex 2X Master Mix (Thermo Scientific, M0536) were used to amplify the donor DNA which was transformed at low concentrations (∼200 ng total). Primers oSLL274, oSLL005 (internal *URA3* primer), and oSLL276 (internal *ARG4* primer) were used to identify heterozygous *URA3* integrations. Single colonies were inoculated in 5 mL of YPD at 30°C with rotation overnight, then plated to 5-FOA. *URA3* loss was confirmed by PCR and candidates were prepared for WGS. For the third strategy, we inoculated single yeast colonies with aneuploid chromosome *VIII* in 5 mL YPD at 30°C with rotation. After ∼24 h of growth, yeast cultures were back-diluted 1:1000 in 5 mL YPD and grown at 30°C with rotation. Back dilutions were repeated for a total of 8 days, then plated on YPD media. Single colonies were selected for WGS preparation.

Minichromosome construction and stability assay

The *CEN8* minichromosome WYYp299 and yeast strain WYYY428 (*MATa his3Δ1 leu2Δ0 met15Δ0 ura3Δ0 ade2Δ ade3Δ trp1Δ63*) were supplied by the Yuen lab.[34] WYYp299 was modified by Gibson assembly to generate the following: a minimal 118-bp *CEN8* construct with no flanking pericentromeric sequences (bSLL50), a construct with 1.5kb of *CDEIII*-flanking pericentromeric sequence (bSLL49), a construct with 500bp of *CDEIII*-flanking pericentromeric sequence (bSLL55), and a construct with 1.5kb of *CDEI*-flanking pericentromeric sequence (bSLL52). All constructs were verified by whole-plasmid, long-read Oxford Nanopore sequencing (Plasmidsaurus, Inc., Eugene, OR). WYYY428 was freshly transformed with all five constructs (including WYYp299) using selection on SC–Uracil plates.

For the minichromosome stability assay, 5 biological replicates were tested per construct. Single colonies were inoculated in 2 mL SC–Uracil overnight at 30°C, then diluted in 5 mL SC–Uracil and grown for 3 doublings to log phase. Cells were plated on SC medium with low adenine (10 μg/mL). After 3 days of growth at 30°C, plates were incubated at 4°C for an additional 3 days to improve visualization of red colony color. Plates were photographed and analyzed using ImageJ. We calculated the total colony area and total red colony area of each plate using Color Threshold and then the Analyze Particles function, keeping parameters constant across all 25 plates. The percentage of red colony area was calculated for each plate, then averaged across the 5 plates for each condition. The standard deviation was also calculated for each construct. Raw data are available in Table S7.

QUANTIFICATION AND STATISTICAL ANALYSIS

Statistical analysis details for the minichromosome stability assay can be found in the corresponding figure legend (Figure 5, in brief) and the methods section. Statistical analyses performed include calculation of the mean and calculation of standard deviation where n = 5 biological replicates per condition, represented by growth of 5 unique colonies inoculated in liquid medium and later plated on solid SC medium with low adenine (see method details). Raw data are provided in Table S7.